

Kinome-wide transcriptional profiling of uveal melanoma reveals new vulnerabilities to targeted therapeutics

Fiona P Bailey¹, Kim Clarke², Helen Kalirai³, Jenna Kenyani³, Haleh Shahidipour³, Francesco Falciani², Judy M Coulson⁴, Joseph J Sacco³, Sarah E Coupland^{3*} and Patrick A Evers^{1*}

¹Department of Biochemistry, Institute of Integrative Biology, University of Liverpool, L69 7ZB, UK

²Computational Biology Facility, Functional and Comparative Genomics, Institute of Integrative Biology, University of Liverpool, L69 7ZB, UK

³Department of Molecular and Clinical Cancer Medicine, Institute of Translational Research, University of Liverpool, L69 3GE, UK

⁴Cellular and Molecular Physiology, Institute of Translational Research, University of Liverpool, L69 3GE, UK

*To whom correspondence should be addressed (sarah.coupland@liverpool.ac.uk) or (Patrick.evers@liverpool.ac.uk)

Running Title: Mitotic protein kinases as promising new targets in human UM

Key words: uveal melanoma, JQ1, transcriptomics, kinase inhibitor, kinome, PLK1, BI6727

Conflicts of Interest: The authors declare no potential conflicts of interest

ABSTRACT

Metastatic uveal melanoma (UM) is invariably fatal, usually within a year of diagnosis. There are currently no effective therapies, and clinical studies employing kinase inhibitors have so far demonstrated limited success. This is despite common activating mutations in *GNAQ/11* genes, which trigger signalling pathways that might predispose tumours to a variety of targeted drugs. In this study, we have profiled kinome expression network dynamics in various human ocular melanomas. We uncovered a shared transcriptional profile in human primary UM samples and across a variety of experimental cell-based models. The poor overall response of UM cells to FDA-approved kinase inhibitors contrasted with much higher sensitivity to the bromodomain inhibitor JQ1, a broad transcriptional repressor. Mechanistically, we identified a repressed FOXM1-dependent kinase sub-network in JQ1-exposed cells that contained multiple cell cycle-regulated protein kinases. Consistently, we demonstrated vulnerability of UM cells to inhibitors of mitotic protein kinases within this network, including the investigational PLK1 inhibitor BI6727. We conclude that analysis of kinome-wide signalling network dynamics has the potential to reveal actionable drug targets and inhibitors of potential therapeutic benefit for UM patients.

SIGNIFICANCE

Therapeutic options for metastatic uveal melanoma (UM) are inadequate, despite molecular lesions in kinase-based signalling networks. Unbiased transcriptional analysis of the entire UM kinome reveals a simple signature that is common to all experimental models and clinical samples. We find that a significant proportion of the UM kinome is transcriptionally down-regulated after exposure to the cytotoxic BET-domain inhibitor JQ1, including a FOXM1-regulated network of mitotic protein kinases. Consistently, targeting of this hub with kinase inhibitors, exemplified by the phase III investigational PLK1 inhibitor BI6727, induces a more selective profile of UM cytotoxicity. Future studies might evaluate the potential therapeutic value of anti-mitotic agents such as BI6727 in metastatic UM.

INTRODUCTION

Uveal melanoma (UM) is the most common primary intraocular malignancy in adults, and arises from neoplastic melanocytes within the middle (vascular) layer in the eye. It is a rare tumour, with an incidence of 5-8 per million individuals per year amongst Caucasian populations (Damato, Eleuteri, Taktak, & Coupland, 2011). Despite successful treatment of the primary tumour by either surgery and/or radiotherapy (Damato, 2012), UM has an enigmatic propensity for metastasis to the liver in up to 50% of patients, and once this occurs, the two year life expectancy is currently only ~8% (Amaro et al., 2017; Carvajal et al., 2017; Diener-West et al., 2005). UM is characterised by activating mutations in α subunits of *GNAQ* or *GNA11* genes in approximately 85% of cases (Van Raamsdonk et al., 2009; Van Raamsdonk et al., 2010), and a lack of *BRAF*, *PI3K* or *NRAS* mutations (Griewank et al., 2012). In contrast, *BRAF* and *NRAS* mutations are common in cutaneous melanomas (Thomas, Edmiston, Alexander, & et al., 2015), where *GNAQ/11* mutations are very rare (Yilmaz et al., 2015). Even less common than UM is its extraocular counterpart conjunctival melanoma (CoM), which occurs in the outer mucous membranes of the eye in 0.2-0.8 per million individuals per year (Kalirai & Coupland). It is also markedly different to UM genetically, being characterised by activating *BRAF* mutations in ~35% of cases (Larsen et al., 2016), and an absence of *GNAQ* or *GNA11* mutations.

Metastatic CoM containing *BRAF* mutations has been treated with some success with *BRAF* kinase inhibitors (Kao, Afshar, Bloomer, & Damato, 2016), although primary or secondary resistance is inevitable, and very few other treatment options are available. In metastatic UM, progress has been slower still (Carvajal et al., 2017), with kinase inhibitors showing very limited clinical efficacy, and no clear improvement in overall survival in phase II trials of the multi-kinase inhibitor sunitinib or the MEK inhibitor selumetinib (Blum, Yang, Komatsubara, & Carvajal, 2016; Carvajal et al., 2014). The therapeutic potential of modulating signalling pathways that lie downstream of constitutively active *GNAQ/11*, such as AKT, PKC, mTOR and the Hippo-YAP pathway is currently being evaluated (Carita et al., 2016; Feng et al., 2014; Shoushtari & Carvajal, 2016; Yu et al., 2014). In addition, targeting cell cycle-regulated protein kinases remains an attractive approach for therapy in a wide range of solid tumours (Otto & Sicinski, 2017), although, to our knowledge, this avenue has not been explored experimentally for metastatic UM.

A complementary (or alternative) therapeutic strategy in UM involves the repression of pro-proliferative transcriptional networks driving growth and survival in tumour cells. Mechanistically, this involves drug-mediated disruption of the interaction between bromodomain-containing proteins, such as BRD4, and acetylated lysine residues on

chromatin-bound histones. Bromodomain Extra Terminal inhibitors (BETi), such as the *MYC*-gene targeting compound JQ1, compete for the acetyl-binding pocket of transcription factors such as BRD4, and block: a) transcription of genes associated with G1/M progression (Dey, Nishiyama, Karpova, McNally, & Ozato, 2009); b) the recruitment of P-TEFb (Bisgrove, Mahmoudi, Henklein, & Verdin, 2007); c) the expression of the master oncogene *MYC* (Delmore et al., 2011); and d) activity of the BRD family themselves (Filippakopoulos et al., 2010). JQ1 is a potent cellular BETi with high selectivity for BET domains of BRD-related transcription factors, particularly bromodomains 1 and 2 of BRD4 (K_d values ~50 nM and ~90 nM respectively). Subsequently, the cytotoxic effects of JQ1 have been reported in a wide number of solid (Bandopadhyay et al., 2014; Cheng et al., 2013; Delmore et al., 2011) and haematological malignancies (Mertz et al., 2011; Ott et al., 2012). JQ1 exhibits extensive repressive effects on proliferative gene expression, and anti-cancer effects are thought to be achieved, in large part, by silencing *MYC*-dependent genes, such as the AP-1 transcription factor *FOSL1* (Baker et al., 2015), and the pro-proliferative Forkhead family member *FOXM1* (Z. Zhang et al., 2016). In both *GNAQ/11*-mutant UM cell lines and a xenografted murine model, JQ1 arrests cell cycle progression in G1 phase *in vitro*, whilst apoptosis in UM is associated with the repression of *Rad51* and *Bcl-xL*-dependent signalling pathways (Ambrosini, Sawle, Musi, & Schwartz, 2015). More recently, dual kinase-bromodomain inhibitors exemplified by the Polo-like kinase (PLK) inhibitors BI-2536 (Scutt et al., 2009; Steegmaier et al., 2007) and BI6727 (Rudolph et al., 2009) have been reported, raising the possibility that these rationally-designed dual inhibitors might have widespread therapeutic potential (Ciceri et al., 2014).

In this paper, we employ kinome-wide transcriptomics to discover a new mRNA expression signature that is shared between human pigmented uveal and conjunctival melanomas, irrespective of *GNAQ/11* or *BRAF* mutational status and chromosome 3 copy number. This kinome 'fingerprint', comprising very low levels of EGFR and high levels of CDK2 mRNAs, is also present in archived patient UM samples and in public data available from the The Cancer Genome Atlas (TCGA) database, where four molecular and clinical UM sub-classes have recently been recognized (Robertson et al., 2017). We also demonstrate that the cytotoxic BETi JQ1 strongly represses a FOXM1-dependent kinase transcriptional network containing cell cycle-related protein kinases in UM cells. Consistently, UM cell lines exposed to investigational anti-mitotic kinase inhibitors were cytotoxic, and selective UM susceptibility to the phase III PLK1 inhibitor BI6727/volasertib was observed. We conclude that kinome-wide analysis of transcription has the potential to expose vulnerabilities in signalling networks for evaluation as novel therapeutic targets in UM patients.

RESULTS

Discovery of a kinome signature in UM and CoM cells

Given the overall low mutational burden in UM, epigenetic mechanisms have recently been proposed to shape the gene transcription networks that regulate UM metastasis (Decatur et al., 2016; Royer-Bertrand et al., 2016). To help understand steady-state and dynamic programmes of transcription in human UM kinomes, we explored mRNA levels in patient samples deposited in TCGA. Principal component analysis (PCA) (Ringner, 2008) was employed to compare variance in whole kinome expression from 80 UM patient samples against a broad panel of distinct tumour samples, including cutaneous melanomas, an ER+/HER2 subset of breast cancer, cervical and colon cancer samples (Figure 1A). This analysis revealed unique clustered kinome expression in all UM samples, which was distinct from other types of tumour sample examined. Interestingly, although UM were most similar to cutaneous melanomas, a clear distinction in kinome profile was still evident between these two tumour types.

Human UM cell lines have been widely employed to compare transcription (An et al., 2011), signalling and drug responses *in vitro* and *ex vivo*. Sequencing of UM cell lines demonstrate common patterns of distinct genomic mutations in *GNAQ/11* and *BAP-1* genes, similar to tumour samples from patients (Supplementary Table 1). These profiles are proving useful as both diagnostic and prognostic markers (Staby et al., 2017). We profiled four well-studied UM cell lines, including 92.1 (derived from a primary UM), which responds to the BETi JQ1 *in vivo* when implanted in a rodent tumour model (Ambrosini et al., 2015), Mel270 (derived from a primary UM), OMM2.5 (a liver metastasis from the same patient as Mel270) and OMM1, a subcutaneous metastasis. In addition, the CoM lines CRMM1 (de Waard, Kolovou, et al., 2015) and CRMM2 (de Waard, Cao, et al., 2015) were compared with model (non-ocular) cancer cell lines, including A375, derived from a cutaneous melanoma. The mutational or expression status of *GNAQ*, *GNA11*, *BRAF* and *BAP-1* (De Waard-Siebinga et al., 1995; Luyten et al., 1996; Verbik, Murray, Tran, & Ksander, 1997) in each cell line is summarised in Supplementary Table 1.

To examine human kinome mRNA expression profiles from experimental UM and CoM cell models, and to identify new potential networks for clinical intervention, we employed NanoString, an unbiased method of mRNA quantification (Kulkarni, 2011). This allowed for the simultaneous measurement of expression dynamics across >500 mRNAs, which together constitute the human kinome, a rich source of drug targets (Bago et al., 2016; Manning, Whyte, Martinez, Hunter, & Sudarsanam, 2002).

Interestingly, whole kinome expression profiles of the ocular melanoma cell lines were closely clustered together, despite differential mutational status of *GNAQ/11* and *BRAF* genes in UM and CoM cell lines. Notably, this pattern was distinct from the *BRAF*-mutated cutaneous melanoma line A375, and all other cell lines examined (Figure 1B). Amongst the ocular melanoma subgroup, discrete kinome clusters were produced that were defined by related cell lines. One kinome cluster included the UM lines Mel270 and OMM2.5, which were derived from the same patient. A second cluster in cell lines 92.1 and OMM1 contained Q209L mutations in the related *GNAQ/11* homologues, and a third comprised the related CoM lines CRMM1 and 2, which differ in their *BRAF* mutational status (Figure 1B).

To deconvolute our whole kinome data, we focused on kinase mRNAs that exhibited differential high or low expression levels in melanoma. We found extremely low levels of EGFR mRNA in all UM and CoM cell lines, (Figure 1C): it was minimally ~50 fold lower in ocular melanoma cells when compared with carcinoma cell lines and the skin melanoma cell line A375. In marked contrast, CDK2 transcript levels were always in the highest 1-2% of kinase mRNAs in all UM (Supplementary Figure 1), and always over-expressed at 2-4 fold higher levels in UM and CoM cell lines (Figure 1C). The mRNA encoding a regulator of MAPK pathways (TAOK3) was also highly expressed in UM and CRMM1 cells when compared to control cells (Supplementary Figure 1). As internal controls, we confirmed that BET-domain containing BRD2 and BRD4 mRNAs were highly expressed in all cells lines examined, with no positive selection in melanoma cells (Supplementary Figure 1). As shown in Figure 1D, and in full agreement with our expression analysis in cells, EGFR mRNA was extremely low, and CDK2 very high, in all 80 human UM examined in the TCGA database. Quantitatively across all the samples, mean expression levels of CDK2 transcripts were ~250-fold higher than those of EGFR (Figure 1D), revealing the enormous range in transcript levels detectable by this approach.

We next established that EGFR protein levels were essentially undetectable in both UM and CoM cells, in contrast to all other cancer cells tested, including a cutaneous melanoma. Conversely, CDK2 protein levels were markedly higher in the same UM and CoM lysates in all the cases examined (Figure 1E), consistent with our transcriptional data.

Next, we evaluated kinome expression profiles in nine formalin-fixed and paraffin-embedded primary UM. Consistently, we observed exceptionally high levels of CDK2 and TAOK3 mRNAs, in contrast to very low expression of EGFR mRNA, and BRD2 and BRD4 mRNA levels were consistently amongst the highest 10% of transcripts examined (Supplementary Figures 2A and 2B). Interestingly, there was no correlation between CDK2 (high) or EGFR

(low) signatures and chromosome 3 status, a known strong prognostic marker in UM (Damato et al., 2011; van Beek et al., 2014), in the samples examined

Our analysis suggests that kinome-wide mRNA data, and in particular, CDK2 and EGFR status, can be used to classify ocular melanoma cell types *in vitro* and *in vivo*, and might form the basis of a predictive network relevant to understanding differential kinase signalling pathways present in UM patients. To examine whether high expression of CDK2 in UM and CoM was predictive for sensitivity to chemical CDK2 inhibition, we exposed UM, CoM and control cancer cell lines derived from non-ocular sites to the pre-clinical CDK2 inhibitor SNS-032, the subject of a Phase 1 clinical trial (Tong et al., 2010). By comparing cell viability, we observed a broad, non-specific, inhibitory effect (SNS-032 EC₅₀ 60-400 nM) in all cells tested irrespective of CDK2 mRNA or protein levels (Supplementary Figure 3A).

Moreover, the clinically approved selective CDK4/6 inhibitor palbociclib (Whittaker, Mallinger, Workman, & Clarke, 2017) exhibited a wide range of toxicity across all UM and CoM cell lines tested, indicating that its efficacy did not correlate with GNAQ/11 mutational status, or uveal compared to conjunctival origin (Supplementary Figure 3B).

Comparing responses of ocular melanoma cells to kinase and BET-domain inhibitors

We next assembled a panel of FDA-approved inhibitors, including specific and pan-tyrosine kinase inhibitors (TKIs) and the UM candidate selumetinib (Komatsubara, Manson, & Carvajal, 2016) and calculated EC₅₀ values associated with cell killing. As expected, UM and CoM demonstrated limited sensitivity (EC₅₀ values >1 μM) to a variety of TKIs, including those targeting EGFR, whose expression is extremely low in these cells (Figure 1C). Interestingly, the MEKi selumetinib exhibited higher cytotoxicity towards UM cells, particularly those derived from primary tumours (92.1 and Mel270), with mean EC₅₀ values lying in the submicromolar range. Of note, CoM cell lines were also relatively sensitive to the non-specific TKI ponatinib, in contrast to all UM cell lines examined. As a positive control BCR-ABL-positive K562 CML cells exhibited low nanomolar sensitivity to approved clinical TKIs (Figure 2A), whose marked lack of effect in any UM cells was prominent, consistent with experimental clinical findings detailing a lack of imatinib response in KIT-positive UM (Calipel et al., 2014).

The resistance of tumour cells to kinase inhibitors can sometimes be overcome by exposing them to cellular BET domain inhibitors such as JQ1 (Kurimchak et al., 2016; Stuhlmiller et al., 2015). We therefore turned our attention to chemical targeting of Bromodomain (BRD) proteins, which are known to regulate expression of oncogenic *MYC* (Delmore et al., 2011) that is frequently upregulated in UM. Chromosome 8q amplification, which encompasses the oncogenic *MYC* locus, is consistently observed in ~30% of UM patients (Caines et al.,

2015; Parrella, Caballero, Sidransky, & Merbs, 2001). Patients with UM characterised by monosomy 3 and amplified 8q have a statistically-significantly higher risk of developing metastatic disease (Damato et al., 2011; van Beek et al., 2014). This risk is enhanced further should additional poor prognostic factors be present, such as ciliary body location, epithelioid cell type, high mitotic count, and extraocular extension (Damato et al., 2011). A recent study concluded that *GNAQ/11* mutations conferred single agent sensitivity to JQ1, which potently represses *MYC* transcription in *GNAQ/11*-mutated UM (Ambrosini et al., 2015). These observations suggested that *MYC* and/or *GNAQ/11* mutational status may be important for the cellular response to broad transcriptional repressors such as JQ1. The very high levels of BRD2 and BRD4 mRNA observed in both UM and CoM cell lines and patient samples (Supplementary Figures 1 and 2) prompted us to test the effect of the BET-domain inhibitor JQ1 and JQ1(-), an inactive enantiomer, across UM, CoM and non-ocular cell types. As shown in Figures 2A and 2B, all UM-derived cells tested were sensitive to JQ1, but not JQ1(-), exhibiting EC_{50} values < 500 nM. In addition, we found that the CoM cell lines CRMM1 and CRMM2 (WT at *GNAQ/11* loci, Supplementary Table 1) were also sensitive to JQ1-induced cell death (Figures 2A and 2B). Interestingly, A375 and colorectal HCT116 cells were relatively resistant to JQ1, with calculated EC_{50} values of >10 μ M and 2.4 μ M respectively, suggesting a potential therapeutic window in UM and CoM for small molecules that interfere with signalling pathways controlled by BRD4 dependent transcription.

Bioinformatic and pathway analysis of kinase signalling pathways in UM

Very little is known about *dynamic* intracellular signalling networks in UM that might contribute to the resistance or sensitisation mechanisms to drugs established in other cancer cell models (Kurimchak et al., 2016; Stuhlmiller et al., 2015). For example, JQ1 has been demonstrated to modulate transcription in proliferative signalling pathways and decrease tumour volume in a mouse xenograft *GNAQ*-mutant model, which coincides with down-regulation of the anti-apoptotic protein Bcl-XL (Ambrosini et al., 2015). As shown in Figure 3A, JQ1 exposure caused a highly significant (>2 fold) downregulation of ~ 100 kinase mRNAs (representing between 17-24% of the total kinome) in all four UM cell lines examined. In contrast, CRMM1/2 cell responses were characterised by up- and down-regulation of relatively few kinase mRNAs. Interestingly, the whole-kinome response of A375 cells resembled the UM kinome response following exposure to JQ1, despite the limited cytotoxicity demonstrated by JQ1 in this cell line.

We next evaluated expression dynamics in the context of cancer signalling pathways, which has the potential to reveal novel single-agent or combinatorial opportunities for therapeutic

intervention, which might avoid unwanted 'off-target' effects of very broad transcriptional repressors such as JQ1. Ingenuity pathway analysis (IPA) confirmed that JQ1 effects were predicted to reduce signalling activity within a variety of proliferative/pro-survival pathways in UM, but not CoM, cells (Figure 3B). These include protein kinases that are specifically associated with metastatic HGF/c-Met, G α Q, NF- κ B and melanocyte-specific signalling pathways. In addition, and consistent with the ability of JQ1 to reduce cell viability (Figure 2) and promote apoptosis (Ambrosini et al., 2015), we noted a prominent number of kinase mRNAs associated with cell death signalling in each of the UM cell lines. In contrast, pathway responses were reversed in JQ1-exposed CoM cells CRMM1 and CRMM2 (Figure 3B), despite an equal cellular sensitivity to JQ1 *in vitro* (Figure 2A). As noted above, IPA analysis of A375 cell response following JQ1 exposure revealed close pathway similarities to those induced in UM cells, despite a lack of cellular toxicity to this compound.

JQ1 reduces the expression of BRD4 and C-MYC in UM cells

We confirmed JQ1 target-engagement and downstream effects in UM cells, by measuring effects on BRD family mRNA (Figure 4A) and evaluating cell cycle distribution (Supplementary Figures 4B and 4C). Together these revealed a JQ1-induced enrichment of UM cells in G1 phase of the cell cycle. At 0.5 μ M JQ1 (\sim EC₅₀ value), there was also a significant reduction in the levels of BRD4 mRNA (red) in all UM cell lines examined, consistent with repression of BRD family transcription, which occurs through blockade of a positive feedback loop (Delmore et al., 2011). Interestingly, CRMM1 and A375 cells responded similarly to UM cell lines in terms of BRD4 repression. This was in contrast to CRMM2 and HCT116 cells, where low micromolar concentrations of JQ1 either increased the levels of BRD2 and BRD4 (CRMM2) or had no significant effect (HCT116). In GNAQ mutant UM cells, the transcript levels of BRD2 decreased following JQ1 exposure, whereas in GNAQ WT cell lines, JQ1 caused a significant increase in the level of BRD2 mRNA. Consistently, c-MYC protein expression was also reduced (Figure 4B) in cell lines exhibiting a reduction in BRD4 mRNA (Figure 4A). In agreement with our cell cycle analysis, mRNA levels of the MYC transcriptional target CDK4 (Hermeking et al., 2000), which is involved in G1 progression, were also reduced following JQ1 exposure (Supplementary Figure 4A). Despite BRD4 engagement in both ocular and cutaneous melanoma cell types, no correlation between target engagement and subsequent cell death could be established for JQ1. This finding is in line with a recent report (Ambrosini et al., 2015), where JQ1-regulated c-MYC expression was broadly repressed across all UM samples, whereas apoptosis was only observed in a subset of GNAQ mutant cell types.

JQ1 down-regulates a FOXM1-dependent network of protein kinase mRNAs

To evaluate new potentially druggable responsive signalling pathways involved in JQ1-induced cell death that might be of relevance to inform UM patient therapeutics, we used the Reconstruction of Transcriptional Networks (RTN) pipeline to evaluate signalling modules (Fletcher et al., 2013). Kinome-wide mRNA expression data were assembled from 80 UM samples in the TCGA database, and compared with kinases identified following JQ1 treatment of UM cell lines (Figure 3A). This analysis demonstrated a very strong positive correlation between mRNA targets of the Forkhead family transcription factor FOXM1 (Alvarez-Fernandez et al., 2010; Fu et al., 2008) and multiple cell cycle-regulated mitotic kinases (Figure 5A). This group included *AURKA* (Figure 5B), *AURKB* (Figure 5C), *PLK1* (Figure 5D) and *BuBR1/BUB1B* (Figure 5E), (but not *CDK2*, Figure 5F), whose important roles as guardians of mitotic entry, progression and exit have established them as potential oncology targets.

Interestingly, the expression of FOXM1-dependent mitotic kinase mRNAs was consistently down-regulated following JQ1 exposure in all four UM cell lines and in A375 cells (Figure 5G, blue shading). In contrast, both up and down-regulation of mitotic kinase mRNAs was observed in response to JQ1 in CoM lines CRMM1 and CRMM2 (Figure 5G). Consistently, JQ1 exposure led to a potent reduction in the levels of FOXM1 protein expression in the three UM cell lines where it could be detected (Figure 5H), similar to effects in *BRAF*-mutant CRMM1, and more apparent than those in *BRAF*-wt CRMM2 cells (Figure 5H). To gain further insight into the JQ1-regulated FOXM1 regulatory network, we performed individual FOXM1 and BRD4 siRNA knockdown in Mel270 and A375 cells and analysed effects on PLK1 mRNA levels by RT-PCR. As shown in Figure 5I, FOXM1 siRNA decreased FOXM1 mRNA >3-fold compared to scrambled siRNA controls, and this was accompanied by a >2.3-fold decrease in PLK1 mRNA levels in Mel270 cells. In the same cell line, knockdown of BRD4 was accompanied by a small, but reproducible, decrease in PLK1 mRNA levels. In A375 cells, FOXM1 or BRD4 knock-down was also accompanied by a small decrease in PLK1 mRNA levels. Importantly, individual knock-down of either BRD4 or FOXM1 in Mel270 cells led to a marked effect on PLK1 protein levels 48h after transfection, in contrast to A375 cells, where neither siRNA altered the total levels of PLK1 (Figure 5J). A temporal correlation between FOXM1 and PLK1 protein expression was previously reported during cell cycle progression in human cells (H. J. Park, Costa, Lau, Tyner, & Raychaudhuri, 2008), and the human PLK1 promoter is a known transcriptional target for the cancer-associated FOXM1 pathway (Chen et al., 2013; Raychaudhuri & Park, 2011).

Targeting the FOXM1-transcription network with kinase inhibitors

Our finding that JQ1 reduced UM cell viability and down-regulated *FOXM1*-regulated kinases suggested a new approach to target proliferative signalling in UM. We hypothesised that chemical repression of the activity of protein kinases in this network might be employed to mimic the widespread and potentially non-specific effects observed with JQ1. We therefore exposed UM, CoM, A375 and HCT116 cells to chemically distinct inhibitors of PLK1, including GSK461364 (Ferrarotto et al., 2016), BI6727/volasertib (Van den Bossche et al., 2016), the dual PLK1-BRD4 inhibitor BI2536 (Mross et al., 2012) and the investigational Aurora B inhibitor (AZD1152, barasertib (Wilkinson et al., 2007)). Cytotoxicity and cell viability were determined by combined SRB and MTT assay (Figure 6A and Supplementary Figure 5), employing JQ1 and the BRAF V600E inhibitor vemurafenib as experimental controls. As shown in Figure 6A, GSK461364, BI2536 and AZD1152 all exhibited non-selective cytotoxicity, with mean EC_{50} values <20 nM (Figure 6A). Interestingly, BI6727 demonstrated clear selectivity in this assay, with low nanomolar cytotoxicity in UM lines, in comparison to other cell types examined, including *BRAF*-mutant A375 (~ 1 μ M) and CRMM1 CoM (650 nM) cell lines, which both exhibited hypersensitive to vemurafenib. These findings were confirmed by clonogenic assays, which showed specific effects of BI6727 on UM cells (Figure 6B). Finally, when kinome-wide transcriptional responses to BI6727 in the UM cell line 92.1 were compared with the BETi JQ1 (Supplementary Figure 6B), clear mechanistic differences between the two compounds became apparent. For example, BI6727 had no effect on BRD4 mRNA levels or members of the *FOXM1*-regulated mRNA network that are down-regulated by JQ1. This finding is consistent with recent data suggesting that BI6727 only binds to the BET domain of BRD4 in cells at concentrations two to three orders higher than the EC_{50} value established here (Gjertsen & Schoffski, 2015). The mechanism of BI6727 cytotoxicity in UM cell lines, therefore, appears to be distinct from that of JQ1 and the dual-PLK1/BETi BI2536, which we propose might underlie the window of selectivity identified in UM cells.

DISCUSSION

In this study, we undertook a transcriptomic and chemical biology approach to evaluate the human kinome in two rare melanomas that arise either in the uveal tract (UM) or conjunctival membranes (CoM) of the eye. These melanomas receive less attention than metastatic cutaneous melanomas, whose mutational status has been exploited clinically with targeted BRAF kinase inhibitors. We focused on increasing our understanding of cellular protein kinase networks, since they represent important (but currently ineffective) druggable modules in metastatic UM downstream of mutated $G\alpha$ -subunits of *GNAQ/GNA11*. The importance of an unbiased understanding of kinome dynamics to guide therapeutic options is made clear by a recent dissection of responses to targeted kinase therapies in breast cancer models (Bago et al., 2016), and made relevant to UM by the recent discovery of pathway-specific kinase inhibitors in human pre-clinical models (Carita et al., 2016).

A multiplexed approach to simultaneously quantify mRNA expression of the entire human kinome in samples from four UM and two CoM cell lines facilitated the identification of a kinome mRNA signature that was specific to UM and CoM. Several kinase mRNAs are highlighted by our analysis: EGFR, (low expression) and CDK2 and TAOK3 (high expression). In agreement with these findings, EGFR levels have previously been reported to be low or undetectable in immortalized UM cell lines (Amaro et al., 2013). In contrast, Amaro and colleagues reported high levels of EGFR in the cell lines 'Mel285' and 'Mel290'. However, these cells are highly unusual, and do not display the typical antigens associated with melanoma (e.g. MelanA) (Amaro et al., 2013; Griewank et al., 2012; van Dinten et al., 2005). The clinical or signalling relevance of high basal mRNA levels of CDK2 and TAOK3, the latter potentially lying downstream of *GNAQ/11* as a transducer of MAPK pathway signalling in UM, remains unknown, although clear co-segregation of these mRNAs as part of a unique UM signature (Figure 1) might be useful for future diagnostic applications.

CDK2 protein kinase activity is modulated by cancer-associated Cyclin E and p27Kip regulatory partners, and is classically associated with G1/S phase progression. In melanocytes, CDK2 levels are under the control of melanogenesis-controlled transcription factor (MITF) (Du et al., 2004), and we speculate that MITF is also responsible for the high levels of CDK2 observed in ocular melanomas (Figure 1) as previously established in distinct UM models (Yan et al., 2012). Consistent with a general proliferative role for CDK2, all UM and CoM cells studied exhibited sensitivity to the CDK2 inhibitor SNS032, although effects were not nearly as marked as those measured with Aurora B or PLK1 inhibitors. During the course of our studies, we confirmed that selumetinib (a MEKi currently undergoing phase III clinical trials in patients with metastatic UM) was modestly potent at killing cultured UM

cells, including two cell lines derived from metastatic sites (Figure 2A). However, no clear beneficial patient outcome has been observed following a phase II clinical trial of the TKI sunitinib (SUAVE) (Blum et al., 2016; Sacco et al., 2013) or evaluation of selumetinib alongside the alkylating agent temozolomide, where 97% of patients treated with selumetinib suffered adverse effects, with 37% requiring reductions in dosage, with little improvement in progression free survival and none in overall survival reported (Carvajal et al., 2014).

Although JQ1 has not yet been tested as a targeted clinical agent in UM, this BETi exhibits very broad anti-cancer effects, and has previously demonstrated inhibition of tumour growth in an animal model (Ambrosini et al., 2015), consistent with high levels of transcriptional repression revealed in our UM study (Figures 3 and 5). We extend these published findings by demonstrating that CoM cell models also exhibit sub-micromolar sensitivity to JQ1, despite *GNAQ/11*-wt status and the presence of a *BRAF* mutation in CRMM1, which sensitises these cells to the V600E-selective BRAF inhibitors PLX4720 (Riechardt et al., 2015) and vemurafenib (PLX4032) (Figure 6A). When enrichment for mRNAs in specific canonical pathways and their associated cellular functions were analysed, the likely functional consequences on cell survival and proliferative mechanisms through kinome reprogramming by JQ1 in UM and CoM cells became apparent (Figure 3B). Interestingly, although each of these ocular melanoma models were sensitive to similar concentrations of JQ1 *in vitro* (Figure 2), the 'downstream' transcriptional effects on cell cycle, proliferation and apoptotic kinase networks were essentially reversed in CoM cells. These findings suggest that the specific mechanism of cell killing by JQ1 may vary between melanomas of different cellular origin, rather than simply as a function of *GNAQ/11* status (Ambrosini et al., 2015).

A JQ1-responsive transcriptional network that influences UM cell survival

The presence of a JQ1-regulated FOXM1 transcriptional network in model UM cells was further evaluated to reveal a similar strong correlation in UM patient samples between absolute levels of FOXM1 mRNA, and that of the same family of proliferative protein kinases. CDK1, PLK1, Aurora A and Aurora B are individually rate-limiting for mitotic entry, satisfaction of components of the spindle assembly checkpoint and mitotic exit (Nigg, 2001; Otto & Sicinski, 2017). In agreement with our analysis (Figure 5), BRD4 siRNA phenocopies JQ1 exposure in UM (Ambrosini et al., 2015) and BRD4 siRNA potently suppresses Aurora B mRNA and protein (You et al., 2009). JQ1 has recently been shown to control a transcriptional FOXM1 network in ovarian cancer cells (Z. Zhang et al., 2016), and also controls expression of cell cycle genes such as murine PLK1 (Matzuk et al., 2012) *in vivo*. Kinome-wide signatures obtained with clinical and publicly-available (TCGA) UM patient samples demonstrated that the FOXM1-regulated network contains a number of druggable

protein kinases, including Aurora A, Aurora B and PLK1, all of which have previously been targeted with small molecules in haematological and solid tumours. Based on our analysis of this UM-responsive kinome network, and a direct association with JQ1-induced cell death in UM and CoM cell lines (including the pre-metastatic UM cell line Mel270 and corresponding metastatic cell line derived from the same patient, OMM2.5), we hypothesised that chemical inhibition of the catalytic activity of these mitotic kinases might also kill UM cells. Strikingly, we found that the specific Aurora B inhibitor AZD1152 (barasertib), which exhibits antitumour efficacy in clinical indications (Girdler et al., 2006) and the PLK1 inhibitor GSK461364, both possess cell killing activity at nanomolar concentrations in all cell types tested. In contrast, the phase III PLK1 inhibitor BI6727 (volasertib), which received FDA breakthrough therapy designation in 2013 (Van den Bossche et al., 2016), was as effective at killing UM cells *in vitro* as GSK461364 and AZD1152, and also demonstrated a window of selectivity over other cell types when analysed using complementary experimental approaches (Figure 6).

Relevance of kinome profiling to future clinical strategies in UM

Our analysis raises the possibility that comparative kinome profiling of patient-derived samples could also be employed as a prognostic or predictive tool to help patient profiling in pigmented tumour types, including many UM and CoM. In order to help progress the treatment of metastatic UM, the potential exists for transcriptional profiling to be rapidly taken up as part of experimental and clinical protocols (Barlesi et al., 2016; Mashima et al., 2015; S. M. Park et al., 2016). For example, comparative dynamic kinome profiling between primary and metastatic biopsies from the same patient might reveal cellular dynamics of signalling, and how this becomes subverted by *GNAQ/11* mutations or kinome 'rewiring' during metastatic progression. Such knowledge might enhance the evidence-based testing of drugs as clinical monotherapies or as combinations, whilst permitting direct assessment of drug target engagement, efficacy and kinome-wide responses in patients. Our study demonstrates a transcriptional kinase network controlled by master transcription factors *BRD4*, *MYC* and *FOXM1*, which might be more specifically targeted with antimitotic agents in metastatic UM, where patients remain in urgent need of targeted therapeutic options. Our discovery of a high level of vulnerability of UM cells to the specific PLK1 inhibitor BI6727 (volasertib), suggest new approaches employing anti-mitotic kinase inhibitors to help combat and reduce the metastatic burden in this devastating disease.

MATERIALS AND METHODS

Human subjects and metastatic tumour cell analysis

All primary UM samples were provided by the Ocular Oncology Biobank (Research Ethics Committee Reference 16/NW/0380) as part of a Health Research Authority approved study: Research Ethics Committee Reference 11/NW/0759. The study was conducted in accordance with the Declaration of Helsinki and informed consent was obtained from all human subjects. Total RNA was isolated from approximately 2 x 8 µm sections of tumour cut from formalin fixed paraffin embedded enucleated eyes, using standard techniques with an RNeasy kit (Qiagen), and NanoString analysis of the human kinome and appropriate control housekeeping genes was performed in duplicate.

Cell lines, genotypic and small molecules

Human cell lines derived from human UM (92.1, Mel270, OMM2.5 and OMM1), colorectal carcinoma (HCT116), cervical carcinoma (HeLa), breast cancer (ZR-75-1) and CML (K562) were cultured in RPMI media supplemented with 10% FBS, 100U/ml penicillin and 100 mg/ml streptomycin. The Conjunctival Melanoma (CoM) cell lines CRMM1 and CRMM2 were cultured in F12K media supplemented with 10% FBS containing 100 units/ml penicillin and 100 mg/ml streptomycin. All cells were maintained in a humidified 5% CO₂ atmosphere and genotyped in-house. All UM and CoM cell lines were a kind gift from Professor Martine Jager, Dept Ophthalmology, Leiden University Medical Centre, Leiden, The Netherlands. Cell line *BRAF* mutation status was determined using Qiagen Therascreen *BRAF* RGQ PCR Kit. *GNAQ/GNA11* mutation status was determined by Sanger sequencing. Chromosome 3 and Chromosome 8 status was determined by Multiplex Ligation Dependent Probe Amplification and/or SNP6.0 analysis.

All protein kinase inhibitors were purchased from Selleck Chemicals (Houston, TX, USA), with the exception of imatinib, which was purchased from SignalChem. JQ1 and JQ1- were generous gifts from the SGC-Oxford. All compounds were dissolved in DMSO at 10 mM, and serially diluted in DMSO, unless indicated otherwise.

Cell proliferation, clonogenic assay and cell viability assays

Cells were seeded in a 96-well plate at a density of 4,500 cells/well and left to adhere for 24 hours. Cells were exposed in triplicate to the indicated compound concentration, dissolved in a final concentration of 0.1% (v/v) DMSO. Cell viability and cytotoxicity was determined after 5 days by MTT assay or SRB assay, or after 7 days after fixation and staining in a 1% (w/v) methylene blue, 80% (v/v) methanol solution. Thiazolyl Blue Tetrazolium Bromide (Sigma-

Aldrich, St-Louis, Mo, USA) was dissolved in PBS at a concentration of 5 mg/ml and 5 μ l in 100 μ l media added to the cells for 3 hours. Reactions were stopped by addition of 50 μ l acidified 10% SDS. Absorbance was measured at 570 nm. Cell viability was determined as the percentage of growth compared to control cells (incubated in 0.1% (v/v) DMSO alone), and EC₅₀ values were calculated using GraphPad Prism 6 software using data from three, or occasionally two, independent experiments, each performed in triplicate. Values are mean \pm SD.

NanoString nCounter analysis and RT-PCR

Samples were prepared essentially as described previously (Bago et al., 2016). Briefly, the appropriate cells were collected, counted, washed in PBS and snap-frozen until required. Pellets were thawed and resuspended at a concentration of \sim 6,500 cells/ μ l in RLT buffer (Qiagen). The equivalent of \sim 10,000 cells (\sim 1.5 μ l) was employed for direct kinase mRNA quantification, without the need for further mRNA purification or amplification. mRNAs were hybridised to NanoString human kinome barcode probes and control code sets, and kinase mRNA levels quantified using the nCounter colour barcoding system after count normalisation with internal housekeeping genes and 8 negative controls. For total copy numbers, replicate normalised count values were averaged. *P*-values were calculated using a paired *t*-test (GraphPad Prism software) by comparing treated and control count data for each mRNA. The complete UM kinome datasets are available as Supplementary datasets online. Complete cDNA was generated from total RNA using GoScript Reverse Transcription system (Promega), using 1 μ g RNA per reaction and 0.5 μ g of Random primer. qPCR was performed using a Comparative Ct ($\Delta\Delta$ Ct) method on an Applied Biosystems (AB) StepOnePlus machine, a Power SYBR Green PCR Master Mix and the following primer pairs. PLK1: 5'-AAGAGGAGGAAAGCCCTGAC-3' and 5'-TTCTTCCTCTCCCCGTCATA-3', FOXM1: 5'-TGCAGCTAGGGATGTGAATCTTC-3' and 5'-GGAGCCCAGTCCATCAGAACT-3', BRD4: 5'-CCATGGACATGAGCACAATC-3' and 5'TGGAGAACATCAATCGGACA-3', GAPDH: 5'-TTCACCACCATGGAGAAGGC-3' and 5'-CCCTTTTGGCTCCACCCT-3'. Expression levels were normalized to GAPDH mRNA using AB software.

Cell lysate preparation and Immunoblotting

Cells were collected, washed 3 x in PBS and then lysed in RIPA buffer (1% (v/v) SDS, 1% Tergitol type NP-40, 50 mM Tris (pH 7.4), 150 mM NaCl, 1 x protease inhibitor cocktail tablet (Roche). Cell lysates were sonicated on ice and insoluble matter cleared by centrifugation. Protein concentration was determined using a Pierce BCA Protein Assay Kit and 30 μ g of each sample were denatured in 1X Laemmli sample buffer, heated at 95°C for 5 min and

then analysed by SDS-PAGE using 10% (v/v) polyacrylamide gels. Standard Western blotting procedures were followed. Membranes were incubated with the following primary antibodies MYC (D84C12), cyclin-D1 (#2922), FOXM1 (D12D5), PLK1 (Cell Signaling Technologies) and alpha tubulin (TAT-1, CRUK) overnight. Antibodies were detected with appropriate HRP-conjugated secondary antibodies using ECL.

Computational and Pathway analyses

Computational analysis including PCA and data visualisation was performed using the R software package for statistical computing (<https://www.r-project.org/>) and commercial Ingenuity Pathway Analysis software (QiagenBiosciences).

The RTN pipeline was carried out in R using the RTN package with default parameters. This pipeline is able to reconstruct genome-wide transcriptional networks from microarray or RNA-seq data using an information-based theoretical approach, which it uses to search for network hubs whose first neighbours are enriched with genes provided from a signature provided by the user. Normalised and batch-corrected gene expression data for Uveal Melanoma patients was downloaded from the MD Anderson TCGA MBatch website (<http://bioinformatics.mdanderson.org/tcgambatch/>) and used for the network reconstruction phase. The list of potential network hubs was limited to transcription factors found within the AnimalTFDB 2.0 database (H. M. Zhang et al., 2015). The network shown in Figure 5A represents a consensus of the analyses using gene signatures from the four UM cell lines.

REFERENCES

- Alvarez-Fernandez, M., Halim, V. A., Krenning, L., Aprelia, M., Mohammed, S., Heck, A. J., & Medema, R. H. (2010). Recovery from a DNA-damage-induced G2 arrest requires Cdk-dependent activation of FoxM1. *EMBO Rep*, *11*(6), 452-458. doi:10.1038/embor.2010.46
- Amaro, A., Gangemi, R., Piaggio, F., Angelini, G., Barisione, G., Ferrini, S., & Pfeffer, U. (2017). The biology of uveal melanoma. *Cancer Metastasis Rev*, *36*(1), 109-140. doi:10.1007/s10555-017-9663-3
- Amaro, A., Mirisola, V., Angelini, G., Musso, A., Tosetti, F., Esposito, A. I., . . . Pfeffer, U. (2013). Evidence of epidermal growth factor receptor expression in uveal melanoma: inhibition of epidermal growth factor-mediated signalling by Gefitinib and Cetuximab triggered antibody-dependent cellular cytotoxicity. *Eur J Cancer*, *49*(15), 3353-3365. doi:10.1016/j.ejca.2013.06.011
- Ambrosini, G., Sawle, A. D., Musi, E., & Schwartz, G. K. (2015). BRD4-targeted therapy induces Myc-independent cytotoxicity in Gnaq/11-mutant uveal melanoma cells. *Oncotarget*, *6*(32), 33397-33409. doi:10.18632/oncotarget.5179
- An, J., Wan, H., Zhou, X., Hu, D. N., Wang, L., Hao, L., . . . Qu, J. (2011). A comparative transcriptomic analysis of uveal melanoma and normal uveal melanocyte. *PLoS One*, *6*(1), e16516. doi:10.1371/journal.pone.0016516
- Bago, R., Sommer, E., Castel, P., Crafter, C., Bailey, F. P., Shpiro, N., . . . Alessi, D. R. (2016). The hVps34-SGK3 pathway alleviates sustained PI3K/Akt inhibition by stimulating mTORC1 and tumour growth. *EMBO J*, *35*(17), 1902-1922. doi:10.15252/embj.201693929
- Baker, E. K., Taylor, S., Gupte, A., Sharp, P. P., Walia, M., Walsh, N. C., . . . Walkley, C. R. (2015). BET inhibitors induce apoptosis through a MYC independent mechanism and synergise with CDK inhibitors to kill osteosarcoma cells. *Sci Rep*, *5*, 10120. doi:10.1038/srep10120
- Bandopadhyay, P., Berghold, G., Nguyen, B., Schubert, S., Gholamin, S., Tang, Y., . . . Cho, Y. J. (2014). BET bromodomain inhibition of MYC-amplified medulloblastoma. *Clin Cancer Res*, *20*(4), 912-925. doi:10.1158/1078-0432.CCR-13-2281
- Barlesi, F., Mazieres, J., Merlio, J. P., Debieuvre, D., Mosser, J., Lena, H., . . . Biomarkers France, c. (2016). Routine molecular profiling of patients with advanced non-small-cell lung cancer: results of a 1-year nationwide programme of the French Cooperative Thoracic Intergroup (IFCT). *Lancet*, *387*(10026), 1415-1426. doi:10.1016/S0140-6736(16)00004-0
- Bisgrove, D. A., Mahmoudi, T., Henklein, P., & Verdin, E. (2007). Conserved P-TEFb-interacting domain of BRD4 inhibits HIV transcription. *Proc Natl Acad Sci U S A*, *104*(34), 13690-13695. doi:10.1073/pnas.0705053104
- Blum, E. S., Yang, J., Komatsubara, K. M., & Carvajal, R. D. (2016). Clinical Management of Uveal and Conjunctival Melanoma. *Oncology (Williston Park)*, *30*(1), 29-32, 34-43, 48.
- Caines, R., Eleuteri, A., Kalirai, H., Fisher, A. C., Heimann, H., Damato, B. E., . . . Taktak, A. F. (2015). Cluster analysis of multiplex ligation-dependent probe amplification data in choroidal melanoma. *Mol Vis*, *21*, 1-11.
- Calipel, A., Landreville, S., De La Fouchardiere, A., Mascarelli, F., Rivoire, M., Penel, N., & Mouriaux, F. (2014). Mechanisms of resistance to imatinib mesylate in

- KIT-positive metastatic uveal melanoma. *Clin Exp Metastasis*, 31(5), 553-564. doi:10.1007/s10585-014-9649-2
- Carita, G., Frisch-Dit-Leitz, E., Dahmani, A., Raymondie, C., Cassoux, N., Piperno-Neumann, S., . . . Decaudin, D. (2016). Dual inhibition of protein kinase C and p53-MDM2 or PKC and mTORC1 are novel efficient therapeutic approaches for uveal melanoma. *Oncotarget*, 7(23), 33542-33556. doi:10.18632/oncotarget.9552
- Carvajal, R. D., Schwartz, G. K., Tezel, T., Marr, B., Francis, J. H., & Nathan, P. D. (2017). Metastatic disease from uveal melanoma: treatment options and future prospects. *Br J Ophthalmol*, 101(1), 38-44. doi:10.1136/bjophthalmol-2016-309034
- Carvajal, R. D., Sosman, J. A., Quevedo, J. F., Milhem, M. M., Joshua, A. M., Kudchadkar, R. R., . . . Schwartz, G. K. (2014). Effect of selumetinib vs chemotherapy on progression-free survival in uveal melanoma: a randomized clinical trial. *JAMA*, 311(23), 2397-2405. doi:10.1001/jama.2014.6096
- Chen, X., Muller, G. A., Quaas, M., Fischer, M., Han, N., Stutchbury, B., . . . Engeland, K. (2013). The forkhead transcription factor FOXM1 controls cell cycle-dependent gene expression through an atypical chromatin binding mechanism. *Mol Cell Biol*, 33(2), 227-236. doi:10.1128/MCB.00881-12
- Cheng, Z., Gong, Y., Ma, Y., Lu, K., Lu, X., Pierce, L. A., . . . Wang, J. (2013). Inhibition of BET bromodomain targets genetically diverse glioblastoma. *Clin Cancer Res*, 19(7), 1748-1759. doi:10.1158/1078-0432.CCR-12-3066
- Ciceri, P., Muller, S., O'Mahony, A., Fedorov, O., Filippakopoulos, P., Hunt, J. P., . . . Knapp, S. (2014). Dual kinase-bromodomain inhibitors for rationally designed polypharmacology. *Nat Chem Biol*, 10(4), 305-312. doi:10.1038/nchembio.1471
- Damato, B. (2012). Progress in the management of patients with uveal melanoma. The 2012 Ashton Lecture. *Eye (Lond)*, 26(9), 1157-1172. doi:10.1038/eye.2012.126
- Damato, B., Eleuteri, A., Taktak, A. F., & Coupland, S. E. (2011). Estimating prognosis for survival after treatment of choroidal melanoma. *Prog Retin Eye Res*, 30(5), 285-295. doi:10.1016/j.preteyeres.2011.05.003
- De Waard-Siebinga, I., Blom, D. J., Griffioen, M., Schrier, P. I., Hoogendoorn, E., Beverstock, G., . . . Jager, M. J. (1995). Establishment and characterization of an uveal-melanoma cell line. *Int J Cancer*, 62(2), 155-161.
- de Waard, N. E., Cao, J., McGuire, S. P., Kolovou, P. E., Jordanova, E. S., Ksander, B. R., & Jager, M. J. (2015). A Murine Model for Metastatic Conjunctival Melanoma. *Invest Ophthalmol Vis Sci*, 56(4), 2325-2333. doi:10.1167/iovs.14-15239
- de Waard, N. E., Kolovou, P. E., McGuire, S. P., Cao, J., Frank, N. Y., Frank, M. H., . . . Ksander, B. R. (2015). Expression of Multidrug Resistance Transporter ABCB5 in a Murine Model of Human Conjunctival Melanoma. *Ocul Oncol Pathol*, 1(3), 182-189. doi:10.1159/000371555
- Decatur, C. L., Ong, E., Garg, N., Anbunathan, H., Bowcock, A. M., Field, M. G., & Harbour, J. W. (2016). Driver Mutations in Uveal Melanoma: Associations With Gene Expression Profile and Patient Outcomes. *JAMA ophthalmology*, 134(7), 728-733. doi:10.1001/jamaophthalmol.2016.0903
- Delmore, J. E., Issa, G. C., Lemieux, M. E., Rahl, P. B., Shi, J. W., Jacobs, H. M., . . . Mitsiades, C. S. (2011). BET Bromodomain Inhibition as a Therapeutic

- Strategy to Target c-Myc. *Cell*, 146(6), 903-916. doi:10.1016/j.cell.2011.08.017
- Dey, A., Nishiyama, A., Karpova, T., McNally, J., & Ozato, K. (2009). Brd4 marks select genes on mitotic chromatin and directs postmitotic transcription. *Mol Biol Cell*, 20(23), 4899-4909. doi:10.1091/mbc.E09-05-0380
- Diener-West, M., Reynolds, S. M., Agugliaro, D. J., Caldwell, R., Cumming, K., Earle, J. D., . . . Collaborative Ocular Melanoma Study, G. (2005). Development of metastatic disease after enrollment in the COMS trials for treatment of choroidal melanoma: Collaborative Ocular Melanoma Study Group Report No. 26. *Arch Ophthalmol*, 123(12), 1639-1643. doi:10.1001/archophth.123.12.1639
- Du, J., Widlund, H. R., Horstmann, M. A., Ramaswamy, S., Ross, K., Huber, W. E., . . . Fisher, D. E. (2004). Critical role of CDK2 for melanoma growth linked to its melanocyte-specific transcriptional regulation by MITF. *Cancer Cell*, 6(6), 565-576. doi:10.1016/j.ccr.2004.10.014
- Feng, X., Degese, M. S., Iglesias-Bartolome, R., Vaque, J. P., Molinolo, A. A., Rodrigues, M., . . . Gutkind, J. S. (2014). Hippo-independent activation of YAP by the GNAQ uveal melanoma oncogene through a trio-regulated rho GTPase signaling circuitry. *Cancer Cell*, 25(6), 831-845. doi:10.1016/j.ccr.2014.04.016
- Ferrarotto, R., Goonatilake, R., Young Yoo, S., Tong, P., Giri, U., Peng, S., . . . Johnson, F. M. (2016). Epithelial-Mesenchymal Transition Predicts Polo-Like Kinase 1 Inhibitor-Mediated Apoptosis in Non-Small Cell Lung Cancer. *Clin Cancer Res*, 22(7), 1674-1686. doi:10.1158/1078-0432.CCR-14-2890
- Filippakopoulos, P., Qi, J., Picaud, S., Shen, Y., Smith, W. B., Fedorov, O., . . . Bradner, J. E. (2010). Selective inhibition of BET bromodomains. *Nature*, 468(7327), 1067-1073. doi:10.1038/nature09504
- Fletcher, M. N., Castro, M. A., Wang, X., de Santiago, I., O'Reilly, M., Chin, S. F., . . . Meyer, K. B. (2013). Master regulators of FGFR2 signalling and breast cancer risk. *Nat Commun*, 4, 2464. doi:10.1038/ncomms3464
- Fu, Z., Malureanu, L., Huang, J., Wang, W., Li, H., van Deursen, J. M., . . . Chen, J. (2008). Plk1-dependent phosphorylation of FoxM1 regulates a transcriptional programme required for mitotic progression. *Nat Cell Biol*, 10(9), 1076-1082. doi:10.1038/ncb1767
- Girdler, F., Gascoigne, K. E., Evers, P. A., Hartmuth, S., Crafter, C., Foote, K. M., . . . Taylor, S. S. (2006). Validating Aurora B as an anti-cancer drug target. *J Cell Sci*, 119(Pt 17), 3664-3675. doi:10.1242/jcs.03145
- Gjertsen, B. T., & Schoffski, P. (2015). Discovery and development of the Polo-like kinase inhibitor volasertib in cancer therapy. *Leukemia*, 29(1), 11-19. doi:10.1038/leu.2014.222
- Griewank, K. G., Yu, X., Khalili, J., Sozen, M. M., Stempke-Hale, K., Bernatchez, C., . . . Woodman, S. E. (2012). Genetic and molecular characterization of uveal melanoma cell lines. *Pigment Cell Melanoma Res*, 25(2), 182-187. doi:10.1111/j.1755-148X.2012.00971.x
- Hermeking, H., Rago, C., Schuhmacher, M., Li, Q., Barrett, J. F., Obya, A. J., . . . Kinzler, K. W. (2000). Identification of CDK4 as a target of c-MYC. *Proceedings of the National Academy of Sciences of the United States of America*, 97(5), 2229-2234. doi:DOI 10.1073/pnas.050586197
- Kalirai, H., & Coupland, S. E. An update on ocular melanoma. *Diagnostic Histopathology*, 21(1), 19-25. doi:10.1016/j.mpdhp.2014.11.002

- Kao, A., Afshar, A., Bloomer, M., & Damato, B. (2016). Management of Primary Acquired Melanosis, Nevus, and Conjunctival Melanoma. *Cancer Control*, 23(2), 117-125.
- Komatsubara, K. M., Manson, D. K., & Carvajal, R. D. (2016). Selumetinib for the treatment of metastatic uveal melanoma: past and future perspectives. *Future Oncol*, 12(11), 1331-1344. doi:10.2217/fon-2015-0075
- Kulkarni, M. M. (2011). Digital multiplexed gene expression analysis using the NanoString nCounter system. *Curr Protoc Mol Biol*, Chapter 25, Unit25B 10. doi:10.1002/0471142727.mb25b10s94
- Kurimchak, A. M., Shelton, C., Duncan, K. E., Johnson, K. J., Brown, J., O'Brien, S., . . . Duncan, J. S. (2016). Resistance to BET Bromodomain Inhibitors Is Mediated by Kinome Reprogramming in Ovarian Cancer. *Cell Rep*, 16(5), 1273-1286. doi:10.1016/j.celrep.2016.06.091
- Larsen, A. C., Dahl, C., Dahmcke, C. M., Lade-Keller, J., Siersma, V. D., Toft, P. B., . . . Heegaard, S. (2016). BRAF mutations in conjunctival melanoma: investigation of incidence, clinicopathological features, prognosis and paired premalignant lesions. *Acta Ophthalmol*, 94(5), 463-470. doi:10.1111/aos.13007
- Luyten, G. P., Naus, N. C., Mooy, C. M., Hagemeyer, A., Kan-Mitchell, J., Van Drunen, E., . . . Luider, T. M. (1996). Establishment and characterization of primary and metastatic uveal melanoma cell lines. *Int J Cancer*, 66(3), 380-387. doi:10.1002/(SICI)1097-0215(19960503)66:3<380::AID-IJC19>3.0.CO;2-F
- Manning, G., Whyte, D. B., Martinez, R., Hunter, T., & Sudarsanam, S. (2002). The protein kinase complement of the human genome. *Science*, 298(5600), 1912-1934. doi:10.1126/science.1075762
- Mashima, T., Ushijima, M., Matsuura, M., Tsukahara, S., Kunimasa, K., Furuno, A., . . . Tomida, A. (2015). Comprehensive transcriptomic analysis of molecularly targeted drugs in cancer for target pathway evaluation. *Cancer Sci*, 106(7), 909-920. doi:10.1111/cas.12682
- Matzuk, M. M., McKeown, M. R., Filippakopoulos, P., Li, Q., Ma, L., Agno, J. E., . . . Bradner, J. E. (2012). Small-molecule inhibition of BRDT for male contraception. *Cell*, 150(4), 673-684. doi:10.1016/j.cell.2012.06.045
- Mertz, J. A., Conery, A. R., Bryant, B. M., Sandy, P., Balasubramanian, S., Mele, D. A., . . . Sims, R. J., 3rd. (2011). Targeting MYC dependence in cancer by inhibiting BET bromodomains. *Proc Natl Acad Sci U S A*, 108(40), 16669-16674. doi:10.1073/pnas.1108190108
- Mross, K., Dittrich, C., Aulitzky, W. E., Strumberg, D., Schutte, J., Schmid, R. M., . . . Scheulen, M. E. (2012). A randomised phase II trial of the Polo-like kinase inhibitor BI 2536 in chemo-naive patients with unresectable exocrine adenocarcinoma of the pancreas - a study within the Central European Society Anticancer Drug Research (CESAR) collaborative network. *Br J Cancer*, 107(2), 280-286. doi:10.1038/bjc.2012.257
- Nigg, E. A. (2001). Mitotic kinases as regulators of cell division and its checkpoints. *Nat Rev Mol Cell Biol*, 2(1), 21-32. doi:10.1038/35048096
- Ott, C. J., Kopp, N., Bird, L., Paranal, R. M., Qi, J., Bowman, T., . . . Weinstock, D. M. (2012). BET bromodomain inhibition targets both c-Myc and IL7R in high-risk acute lymphoblastic leukemia. *Blood*, 120(14), 2843-2852. doi:10.1182/blood-2012-02-413021

- Otto, T., & Sicinski, P. (2017). Cell cycle proteins as promising targets in cancer therapy. *Nat Rev Cancer*, *17*(2), 93-115. doi:10.1038/nrc.2016.138
- Park, H. J., Costa, R. H., Lau, L. F., Tyner, A. L., & Raychaudhuri, P. (2008). Anaphase-promoting complex/cyclosome-CDH1-mediated proteolysis of the forkhead box M1 transcription factor is critical for regulated entry into S phase. *Mol Cell Biol*, *28*(17), 5162-5171. doi:10.1128/MCB.00387-08
- Park, S. M., Wong, D. J., Ooi, C. C., Kurtz, D. M., Vermesh, O., Aalipour, A., . . . Gambhir, S. S. (2016). Molecular profiling of single circulating tumor cells from lung cancer patients. *Proc Natl Acad Sci U S A*, *113*(52), E8379-E8386. doi:10.1073/pnas.1608461113
- Parrella, P., Caballero, O. L., Sidransky, D., & Merbs, S. L. (2001). Detection of c-myc amplification in uveal melanoma by fluorescent in situ hybridization. *Invest Ophthalmol Vis Sci*, *42*(8), 1679-1684.
- Raychaudhuri, P., & Park, H. J. (2011). FoxM1: a master regulator of tumor metastasis. *Cancer Res*, *71*(13), 4329-4333. doi:10.1158/0008-5472.CAN-11-0640
- Riechardt, A. I., Maier, A. K., Nonnenmacher, A., Reichhart, N., Keilholz, U., Kociok, N., . . . Gundlach, E. (2015). B-Raf inhibition in conjunctival melanoma cell lines with PLX 4720. *Br J Ophthalmol*, *99*(12), 1739-1745. doi:10.1136/bjophthalmol-2015-306689
- Ringner, M. (2008). What is principal component analysis? *Nat Biotechnol*, *26*(3), 303-304. doi:10.1038/nbt0308-303
- Robertson, A. G., Shih, J., Yau, C., Gibb, E. A., Oba, J., Mungall, K. L., . . . Woodman, S. E. (2017). Integrative Analysis Identifies Four Molecular and Clinical Subsets in Uveal Melanoma. *Cancer Cell*, *32*(2), 204-220 e215. doi:10.1016/j.ccell.2017.07.003
- Royer-Bertrand, B., Torsello, M., Rimoldi, D., El Zaoui, I., Cisarova, K., Pescini-Gobert, R., . . . Rivolta, C. (2016). Comprehensive Genetic Landscape of Uveal Melanoma by Whole-Genome Sequencing. *American journal of human genetics*, *99*(5), 1190-1198. doi:10.1016/j.ajhg.2016.09.008
- Rudolph, D., Steegmaier, M., Hoffmann, M., Grauert, M., Baum, A., Quant, J., . . . Adolf, G. R. (2009). BI 6727, a Polo-like kinase inhibitor with improved pharmacokinetic profile and broad antitumor activity. *Clin Cancer Res*, *15*(9), 3094-3102. doi:10.1158/1078-0432.CCR-08-2445
- Sacco, J. J., Nathan, P. D., Danson, S., Lorigan, P., Nicholson, S., Ottensmeier, C., . . . Marshall, E. (2013). Sunitinib versus dacarbazine as first-line treatment in patients with metastatic uveal melanoma. *Journal of Clinical Oncology*, *31*(15).
- Scutt, P. J., Chu, M. L., Sloane, D. A., Cherry, M., Bignell, C. R., Williams, D. H., & Evers, P. A. (2009). Discovery and exploitation of inhibitor-resistant aurora and polo kinase mutants for the analysis of mitotic networks. *J Biol Chem*, *284*(23), 15880-15893. doi:10.1074/jbc.M109.005694
- Shoushtari, A. N., & Carvajal, R. D. (2016). Treatment of Uveal Melanoma. *Cancer treatment and research*, *167*, 281-293. doi:10.1007/978-3-319-22539-5_12
- Staby, K. M., Gravdal, K., Mork, S. J., Heegaard, S., Vintermyr, O. K., & Krohn, J. (2017). Prognostic impact of chromosomal aberrations and GNAQ, GNA11 and BAP1 mutations in uveal melanoma. *Acta Ophthalmol*. doi:10.1111/aos.13452
- Steegmaier, M., Hoffmann, M., Baum, A., Lenart, P., Petronczki, M., Krssak, M., . . . Rettig, W. J. (2007). BI 2536, a potent and selective inhibitor of polo-like

- kinase 1, inhibits tumor growth in vivo. *Curr Biol*, 17(4), 316-322. doi:10.1016/j.cub.2006.12.037
- Stuhlmiller, T. J., Miller, S. M., Zawistowski, J. S., Nakamura, K., Beltran, A. S., Duncan, J. S., . . . Johnson, G. L. (2015). Inhibition of Lapatinib-Induced Kinome Reprogramming in ERBB2-Positive Breast Cancer by Targeting BET Family Bromodomains. *Cell Rep*, 11(3), 390-404. doi:10.1016/j.celrep.2015.03.037
- Thomas, N. E., Edmiston, S. N., Alexander, A., & et al. (2015). Association between nras and braf mutational status and melanoma-specific survival among patients with higher-risk primary melanoma. *JAMA Oncology*, 1(3), 359-368. doi:10.1001/jamaoncol.2015.0493
- Tong, W. G., Chen, R., Plunkett, W., Siegel, D., Sinha, R., Harvey, R. D., . . . Wierda, W. G. (2010). Phase I and pharmacologic study of SNS-032, a potent and selective Cdk2, 7, and 9 inhibitor, in patients with advanced chronic lymphocytic leukemia and multiple myeloma. *J Clin Oncol*, 28(18), 3015-3022. doi:10.1200/JCO.2009.26.1347
- van Beek, J. G., Koopmans, A. E., Vaarwater, J., de Rooij, J. J., Paridaens, D., Naus, N. C., . . . Kilic, E. (2014). The prognostic value of extraocular extension in relation to monosomy 3 and gain of chromosome 8q in uveal melanoma. *Investigative ophthalmology & visual science*, 55(3), 1284-1291. doi:10.1167/iovs.13-13670
- Van den Bossche, J., Lardon, F., Deschoolmeester, V., De Pauw, I., Vermorcken, J. B., Specenier, P., . . . Wouters, A. (2016). Spotlight on Volasertib: Preclinical and Clinical Evaluation of a Promising Plk1 Inhibitor. *Med Res Rev*, 36(4), 749-786. doi:10.1002/med.21392
- van Dinten, L. C., Pul, N., van Nieuwpoort, A. F., Out, C. J., Jager, M. J., & van den Elsen, P. J. (2005). Uveal and cutaneous melanoma: shared expression characteristics of melanoma-associated antigens. *Invest Ophthalmol Vis Sci*, 46(1), 24-30. doi:10.1167/iovs.04-0961
- Van Raamsdonk, C. D., Bezrookove, V., Green, G., Bauer, J., Gaugler, L., O'Brien, J. M., . . . Bastian, B. C. (2009). Frequent somatic mutations of GNAQ in uveal melanoma and blue naevi. *Nature*, 457(7229), 599-602. doi:10.1038/nature07586
- Van Raamsdonk, C. D., Griewank, K. G., Crosby, M. B., Garrido, M. C., Vemula, S., Wiesner, T., . . . Bastian, B. C. (2010). Mutations in GNA11 in uveal melanoma. *N Engl J Med*, 363(23), 2191-2199. doi:10.1056/NEJMoa1000584
- Verbik, D. J., Murray, T. G., Tran, J. M., & Ksander, B. R. (1997). Melanomas that develop within the eye inhibit lymphocyte proliferation. *Int J Cancer*, 73(4), 470-478.
- Whittaker, S. R., Mallinger, A., Workman, P., & Clarke, P. A. (2017). Inhibitors of cyclin-dependent kinases as cancer therapeutics. *Pharmacol Ther*. doi:10.1016/j.pharmthera.2017.02.008
- Wilkinson, R. W., Odedra, R., Heaton, S. P., Wedge, S. R., Keen, N. J., Crafter, C., . . . Green, S. (2007). AZD1152, a selective inhibitor of Aurora B kinase, inhibits human tumor xenograft growth by inducing apoptosis. *Clin Cancer Res*, 13(12), 3682-3688. doi:10.1158/1078-0432.CCR-06-2979
- Yan, D., Dong, X. D., Chen, X., Yao, S., Wang, L., Wang, J., . . . Tu, L. (2012). Role of microRNA-182 in posterior uveal melanoma: regulation of tumor development through MITF, BCL2 and cyclin D2. *PLoS One*, 7(7), e40967. doi:10.1371/journal.pone.0040967

- Yilmaz, I., Gamsizkan, M., Kucukodaci, Z., Berber, U., Demirel, D., Haholu, A., & Narli, G. (2015). BRAF, KIT, NRAS, GNAQ and GNA11 mutation analysis in cutaneous melanomas in Turkish population. *Indian J Pathol Microbiol*, 58(3), 279-284. doi:10.4103/0377-4929.162831
- You, J., Li, Q., Wu, C., Kim, J., Ottinger, M., & Howley, P. M. (2009). Regulation of aurora B expression by the bromodomain protein Brd4. *Mol Cell Biol*, 29(18), 5094-5103. doi:10.1128/MCB.00299-09
- Yu, F. X., Luo, J., Mo, J. S., Liu, G., Kim, Y. C., Meng, Z., . . . Guan, K. L. (2014). Mutant Gq/11 promote uveal melanoma tumorigenesis by activating YAP. *Cancer Cell*, 25(6), 822-830. doi:10.1016/j.ccr.2014.04.017
- Zhang, H. M., Liu, T., Liu, C. J., Song, S. Y., Zhang, X. T., Liu, W., . . . Guo, A. Y. (2015). AnimalTFDB 2.0: a resource for expression, prediction and functional study of animal transcription factors. *Nucleic Acids Research*, 43(D1), D76-D81. doi:10.1093/nar/gku887
- Zhang, Z., Ma, P., Jing, Y., Yan, Y., Cai, M. C., Zhang, M., . . . Zhuang, G. (2016). BET Bromodomain Inhibition as a Therapeutic Strategy in Ovarian Cancer by Downregulating FoxM1. *Theranostics*, 6(2), 219-230. doi:10.7150/thno.13178

Figure 1

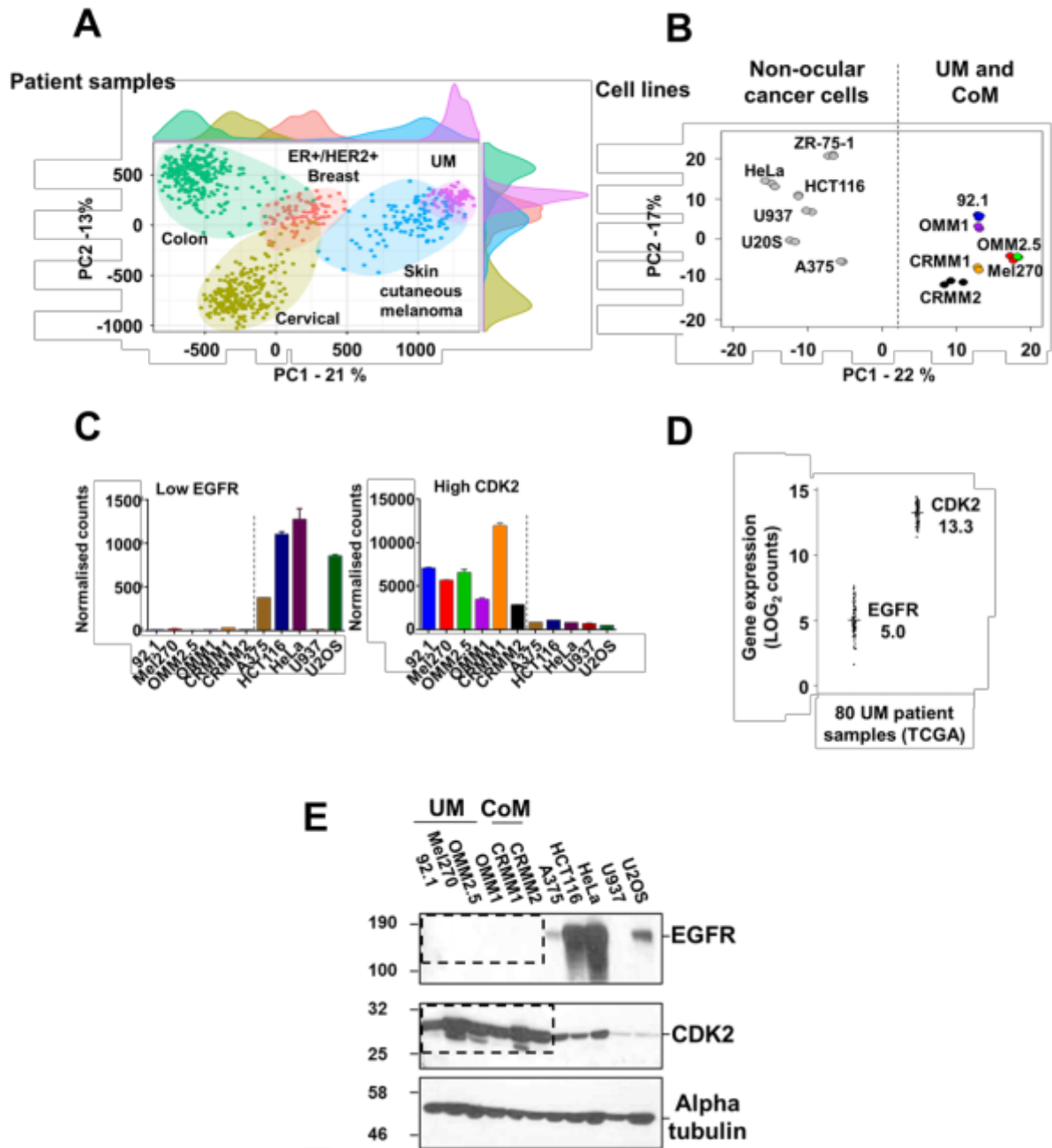


Figure 2

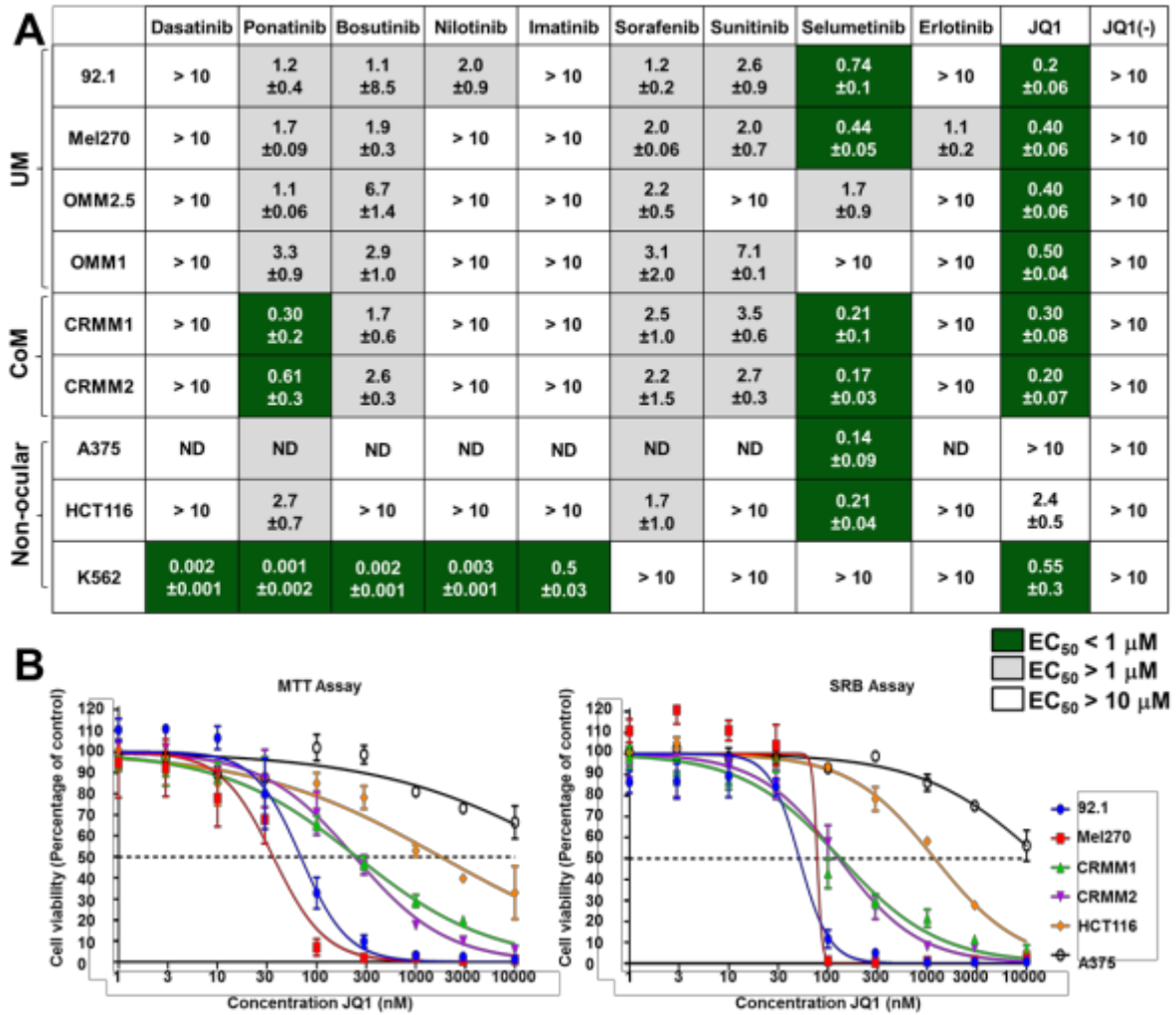
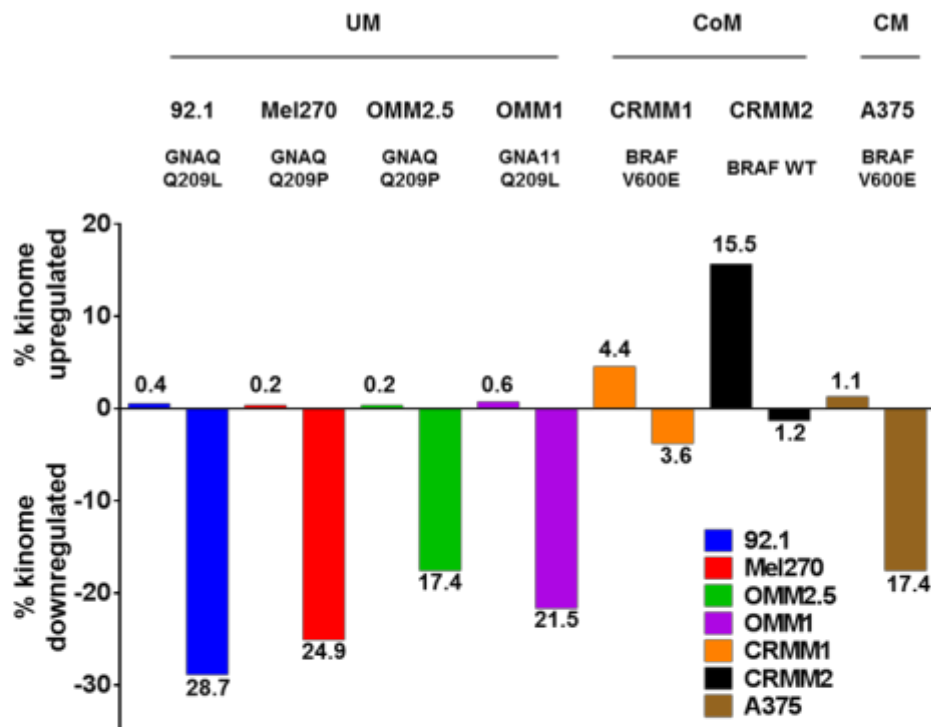


Figure 3

A



B

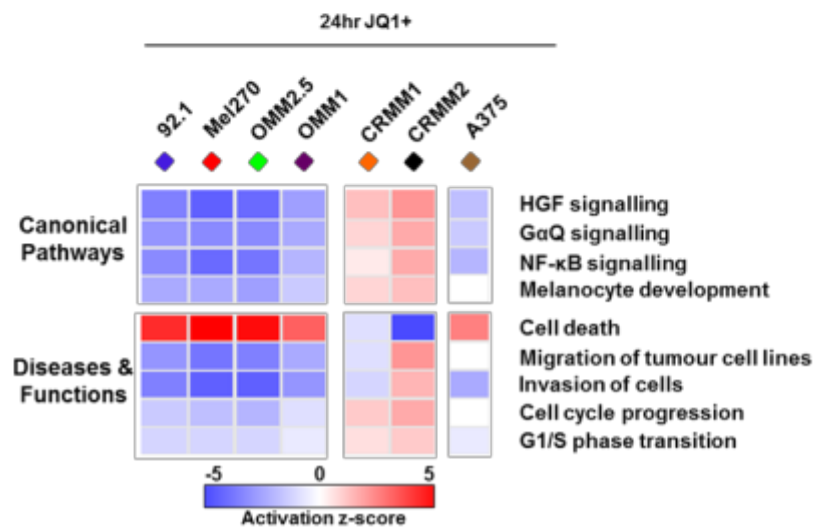


Figure 4

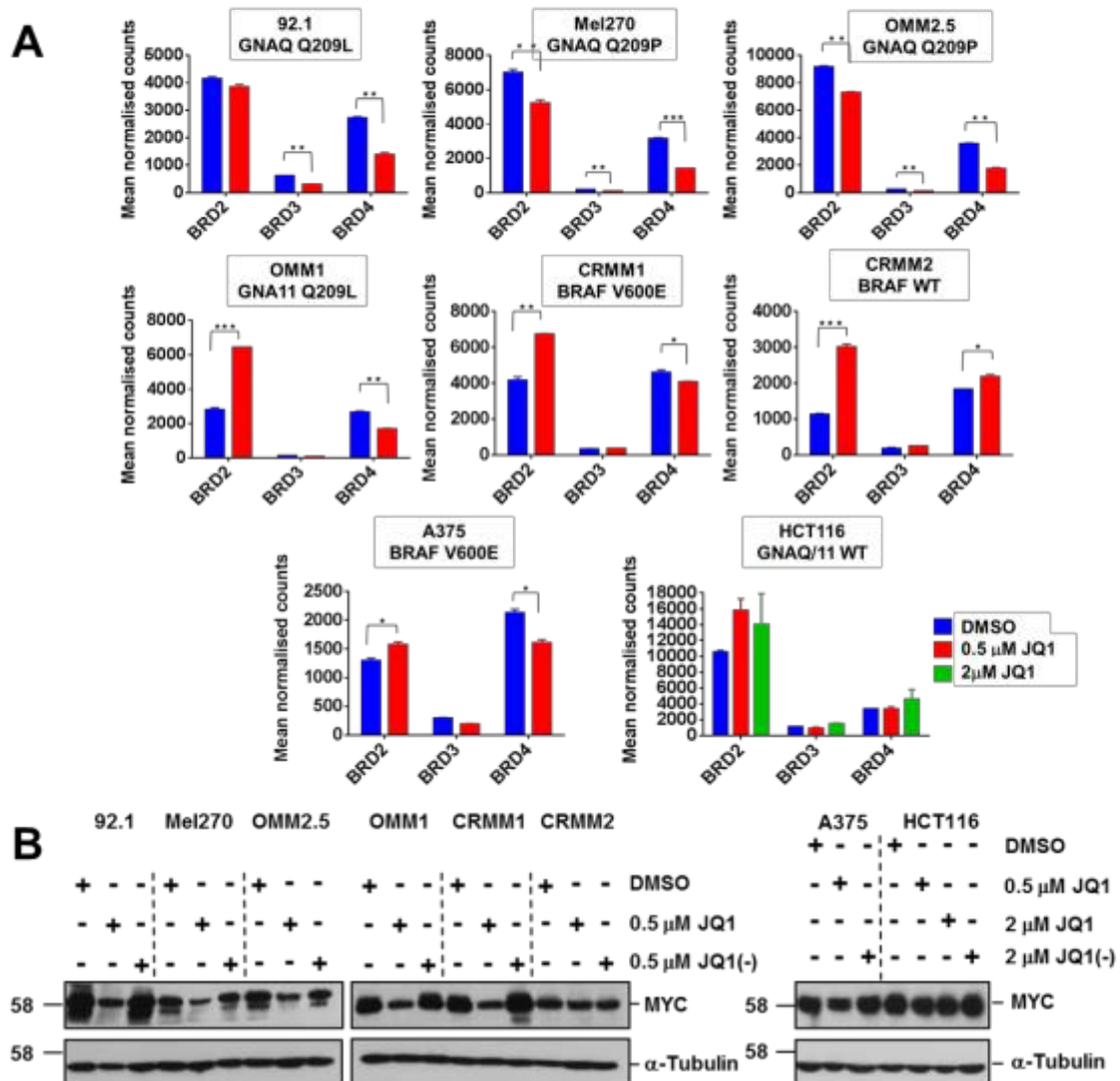


Figure 5

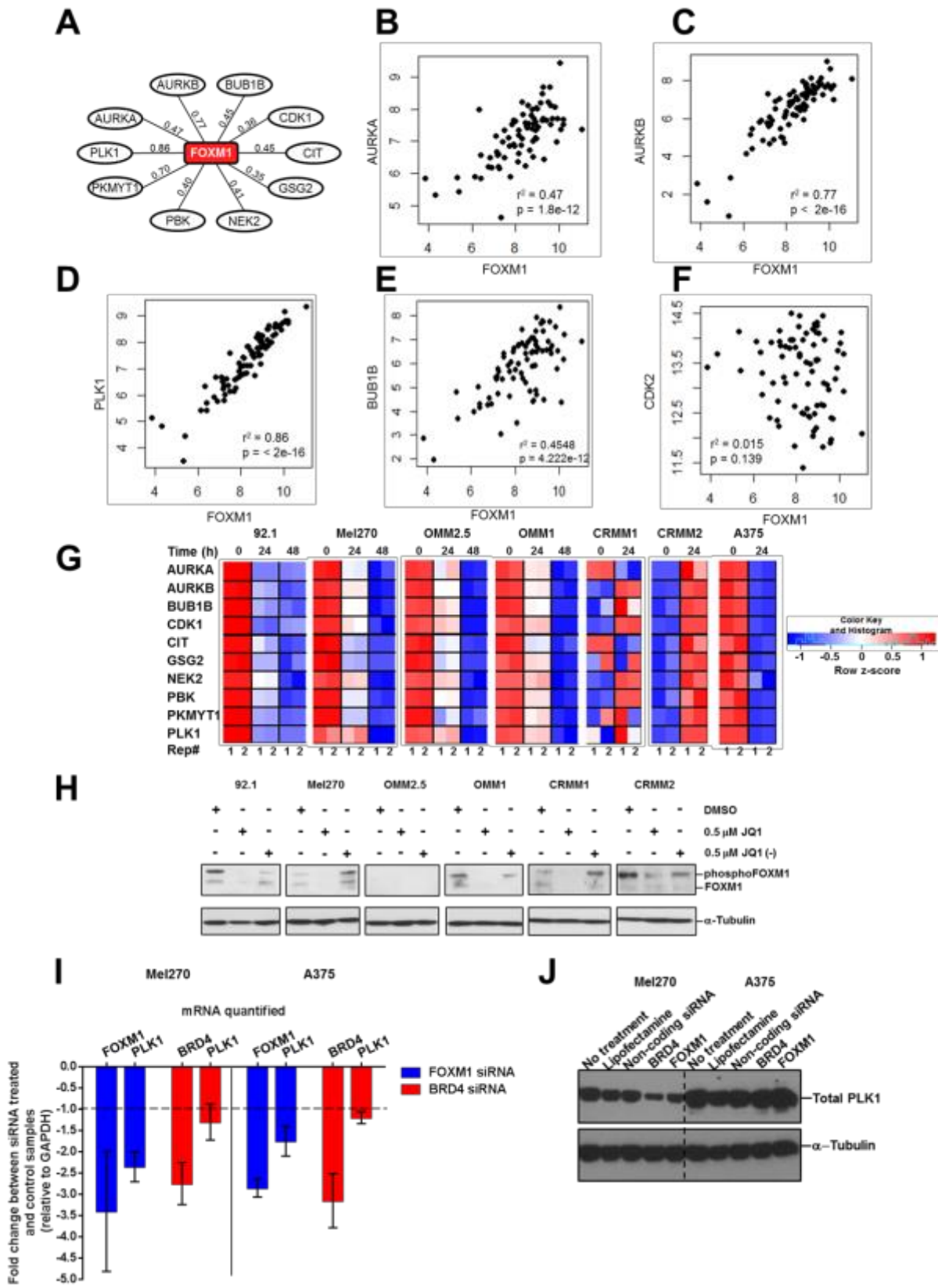


Figure 6

A

EC ₅₀ /nM	GSK461364	AZD1152	BI2536	BI6727	JQ1	VEMURAFENIB
92.1	0.6 ± 0.2	8.8 ± 4.5	2.2 ± 1.1	18.0 ± 4.7	160.3 ± 12.3	8157 ± 789
Mel270	1.2 ± 0.8	2.4 ± 0.3	1.1 ± 1.1	7.5 ± 4.8	345.0 ± 7.1	5478 ± 1376
CRMM1	6.4 ± 0.2	15.2 ± 0.3	4.4 ± 0.0	656.8 ± 373.3	193.4 ± 83.7	619.8 ± 72
CRMM2	0.8 ± 0.7	2.2 ± 0.3	2.3 ± 2.8	91.7 ± 6.5	184.7 ± 79.5	>10000
HCT116	1.7 ± 1.1	3.9 ± 2.6	2.2 ± 1.2	30.7 ± 38.8	1483.5 ± 416.5	>10000
A375	3.9 ± 3.3	3.8 ± 0.8	2.9 ± 0.5	1008 ± 270	>10000	387.9 ± 179

B

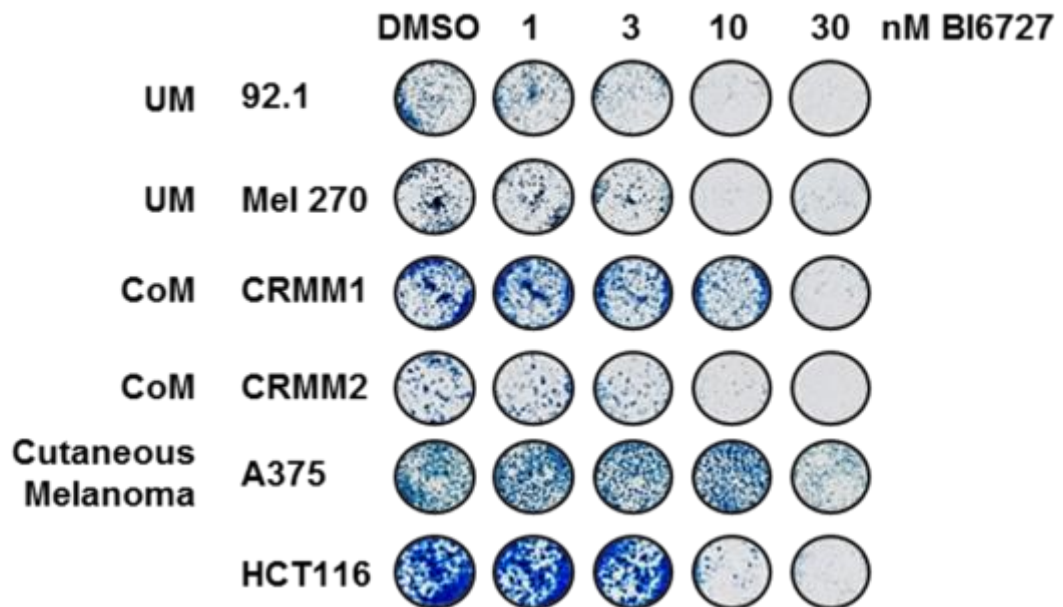


FIGURE LEGENDS

Figure 1. Whole kinome profiling of a panel of human cancer cells

Principal component analysis (PCA) of whole kinome mRNA expression from (A) RNA-Seq patient data from the TCGA, where cancer subtypes are shaded and grouped, and relative data density distribution is plotted on the horizontal and vertical axes and (B) the quantified kinome mRNA from model cell lines measured using NanoString. Note the distinct separation between ocular melanomas and a panel of epithelial and mesenchymal –derived non-ocular cell lines, including the experimental cutaneous melanoma line A375. (C) EGFR and CDK2 mRNA levels were quantified in a panel of cell lines by NanoString. Mean counts for each protein across the UM and CoM, and non-ocular cells have been annotated on the figure. D) Jittered scatter-plot showing relative expression levels of EGFR and CDK2 in human UM patient samples from the TCGA database. The mean expression value (Log_2 scale) is indicated by the horizontal line. E) Analysis of EGFR and CDK2 protein expression levels in RIPA cell lysates. Dashed boxes highlight the ocular melanoma samples. Alpha tubulin was used to confirm similar protein loading.

Figure 2. Assessing the sensitivities of UM to a panel of experimental and FDA-approved kinase and BET-domain inhibitors

(A) Mean EC_{50} values were obtained using MTT cell viability assays (mean \pm S.D. from triplicate assays, $N=2$). The indicated cell lines were incubated with increasing concentrations of the appropriate compound in a range between 10 nM and 10 μM , and compared to 0.1% (v/v) DMSO controls. For ease of analysis, green boxes highlight EC_{50} values $<1 \mu\text{M}$, grey boxes EC_{50} values between 1 μM and 10 μM , and white boxes EC_{50} values $>10 \mu\text{M}$. ND=not determined (B) 4,500 cells were exposed to increasing concentrations of JQ1 and cell viability was determined using MTT and SRB assays.

Figure 3. Quantification of JQ1-induced changes in human kinome mRNA levels in UM and CoM cell lines

(A) Kinome mRNAs were quantified using NanoString technology, following JQ1 exposure and compared to DMSO-treated controls. The number of kinases whose expression changed by more than 2 fold were counted and converted to a percentage of the 522 kinases analysed. Kinases were discarded from the analysis if JQ1(-) caused a similar response (although this was only documented in two cases). Kinases with increased or decreased expression relative to untreated controls are shown on the positive or negative

axis respectively. (B) Ingenuity pathway analysis of the UM and CoM cell lines exposed to JQ1 for 24 hours. Red or blue shaded cells indicate pathways or functional terms that were predicted to be activated or repressed respectively, according to the expression changes observed following JQ1 exposure. Ingenuity pathway analysis provides both a p-value for enrichment of a category as well as a measure of how consistent the fold changes are with increased/decreased activity of that category (z-score). The *least* significant enrichment amongst the categories shown had a p value of < 0.0001.

Figure 4. Confirmation of cellular JQ1 target engagement by transcriptomics

(A) Quantified mRNA counts (mean \pm S.D.) of BRD family members after incubation with DMSO (blue bars) or 500 nM JQ1 (red bars) or 2 μ M JQ1 (green bars). Statistical significance between JQ1-treated cells and the controls was assessed using paired t-tests. *= $p < 0.05$, **= $p < 0.01$, ***= $p < 0.001$. (B) Endogenous *MYC* protein was detected by western blot of lysates exposed to DMSO (control) or the indicated concentrations of JQ1.

Figure 5. Reconstruction of Transcriptional Networks (RTN) analysis: JQ1 mediates expression of a FOXM1-regulated cell cycle kinase network that includes PLK1

(A) Schematic of RTN findings. FOXM1 was predicted to be a key transcription factor that controls a JQ1-dependent transcriptomic kinome signature (adjusted p-value for overlap: 2.0×10^{-6}). A consensus of the putative FOXM1-dependent kinases identified in the analysis are shown in the network. (B-F) Statistical correlation analysis between FOXM1 and (B) AURKA, (C) AURKB, (D) PLK1, (E) BUB1B/BubR1 and (F) CDK2, in the clinical TCGA UM patient cohort (N = 80). (G) Temporal profiling of the putative FOXM1 targets identified by RTN analysis (sample replicates shown). Blue boxes represent a reduction in gene expression, red have increased gene expression. (H) Endogenous FOXM1 protein expression levels were analysed after exposure to the indicated compound (I) PLK1 mRNA levels were quantified by RT-PCR after FOXM1 (blue) or BRD4 (red) siRNA knock-down (48 h) in either Mel270 or A375 cells. (J) PLK1 protein expression levels were analysed by western blotting 48h after control, BRD4 or FOXM1 siRNA transfection protocols in Mel270 or A375 cells. Similar results were seen in an additional experiment.

Figure 6. UM cell lines are highly sensitive to the PLK1 inhibitor BI6727

(A) Cells were exposed to increasing concentrations of the stated compounds. Mean EC_{50} values (nM) were obtained from two independent cell viability assays, SRB and MTT, each performed in triplicate. (B) Colonies formed from single cells were stained with methylene

blue following 7 days exposure to increasing concentrations of BI6727 ranging between 1 nM and 30 nM. DMSO was employed as a mock compound control.

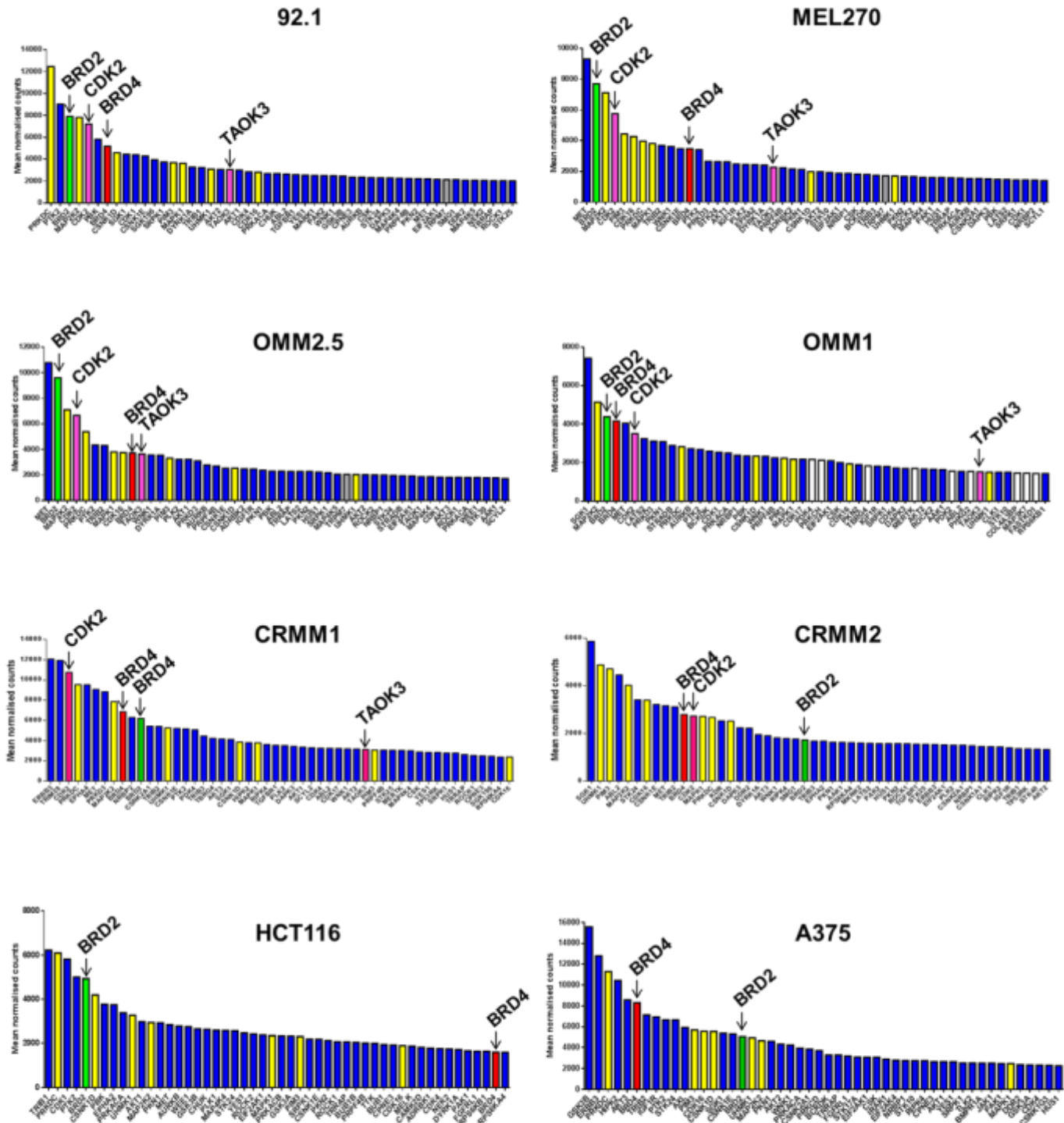
Supplementary Table 1

Characteristics	Cell Line						
	92.1	OMM.1	Mel270*	Omm2.5*	CRMM1	CRMM2	A375
Origin	Primary UM	Subcutaneous UM	Primary UM	Liver UM metastasis	Primary CoM	Primary CoM	Malignant cutaneous Melanoma
Nuclear BAP1	+	+	+	+	ND	ND	ND
Chromosome 3	3pL	ND	N [#]	N	ND	ND	ND
Chromosome 8	G	ND	N [#]	N	ND	ND	ND
GNAQ mutation	c.626 A>T	NMD	c.626 A>C	c.626 A>C	ND	ND	ND
GNA11 mutation	NMD	c.626 A>T	NMD	NMD	ND	ND	ND
SF3B1 mutation	NMD	NMD	NMD	NMD	ND	ND	ND
EIF1AX mutation	c.17 G/A [¥]	NMD	ND	NMD	ND	ND	ND
BRAF mutation	NMD	NMD	NMD	NMD	V600E	NMD	V600E

*Cell lines derived from the same patient; + = present by immunohistochemistry; ND = not determined; NMD = No mutation detected; L = loss; G = Gain; N = Normal; N[#] = copy neutral with LOH

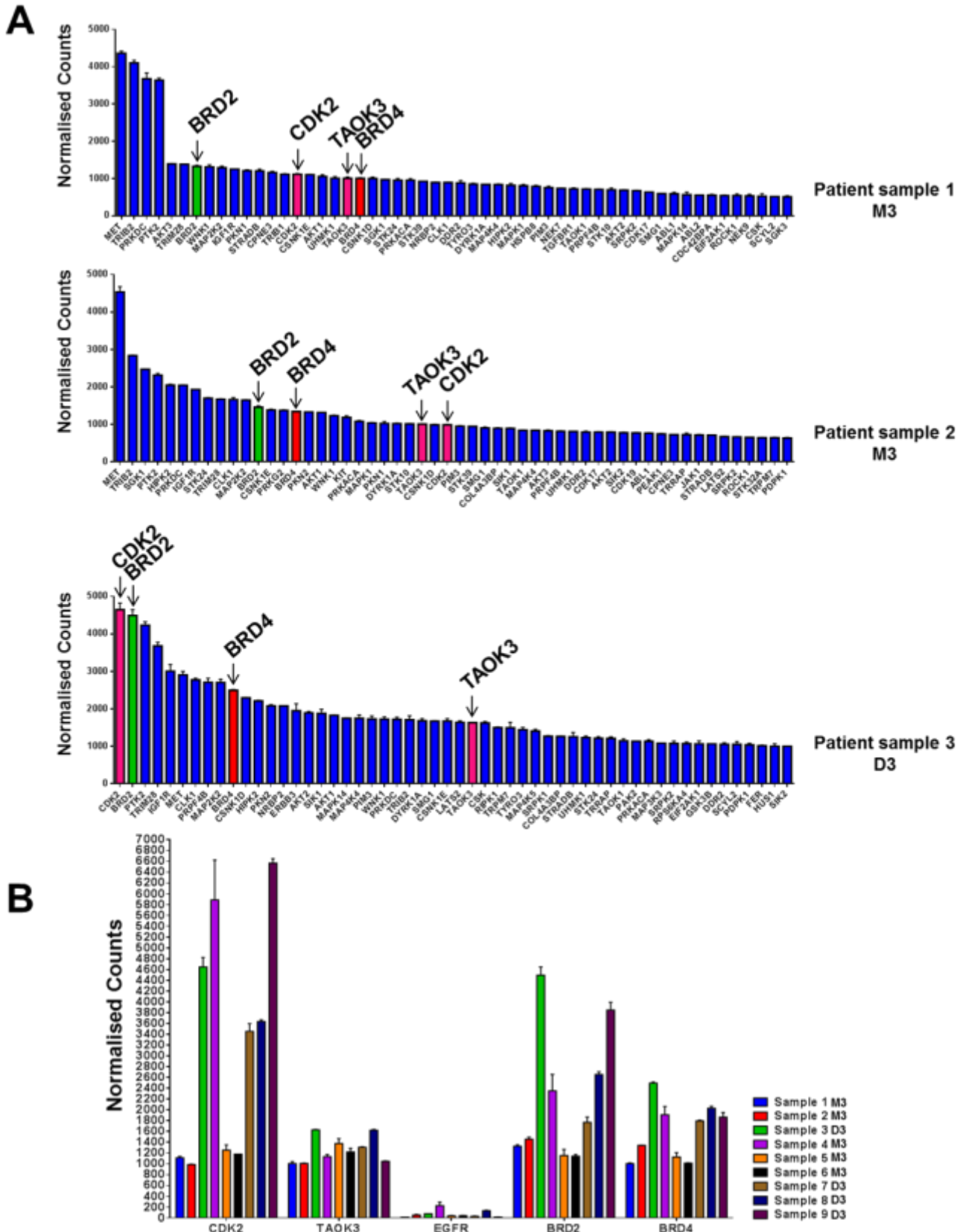
¥ = EIF1AX data taken from Amirouchene-Angelozzi et al, Mol Oncol. 2014 8:1508-20

Supplementary Figure 1

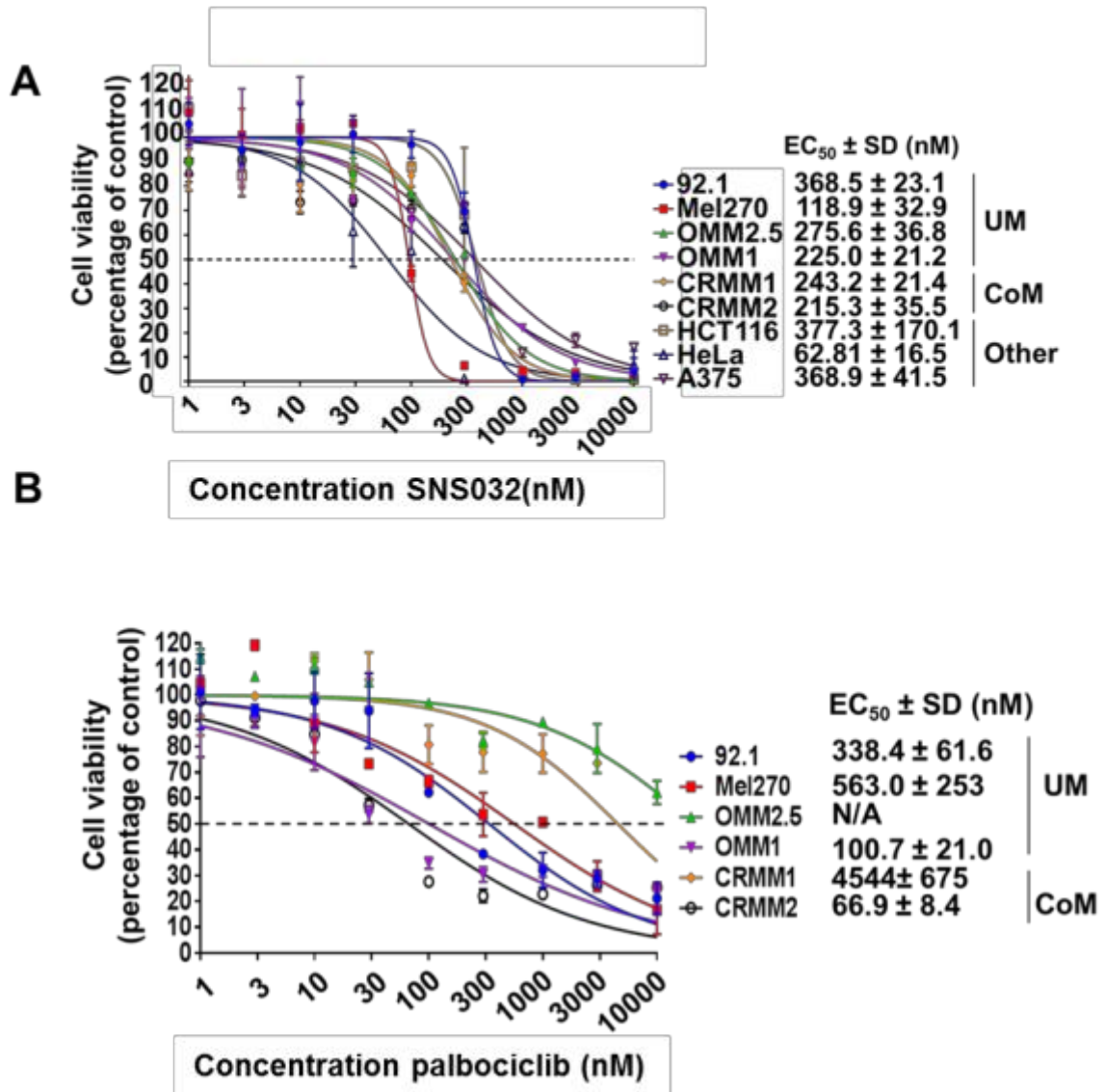


- Highly expressed in all cell lines
- Highly expressed in all UM cell lines
- Highly expressed in GNAQ mutated cell lines
- Highly expressed solely in GNA11 mutated OMM1
- BRD2
- BRD4

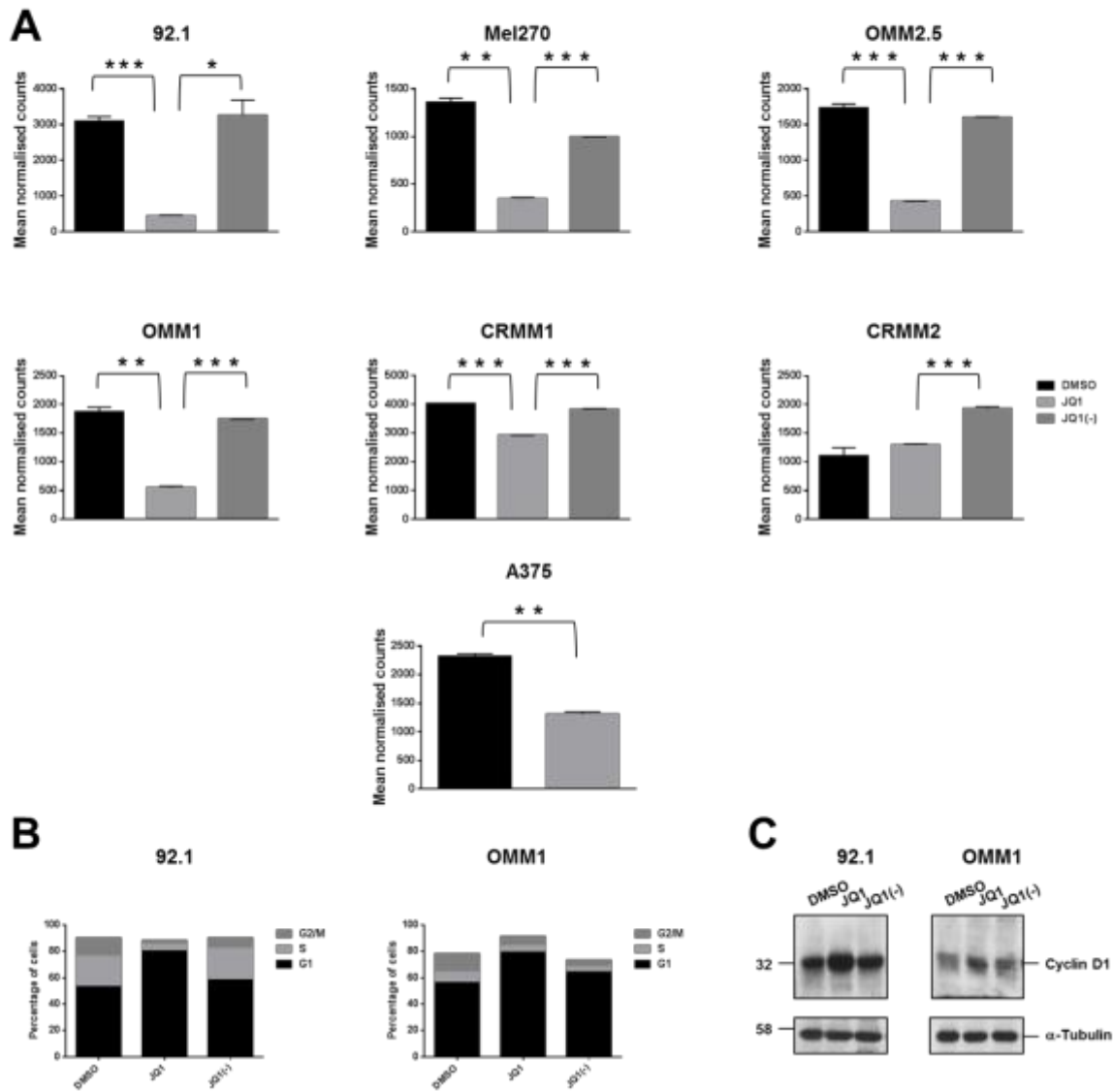
Supplementary Figure 2



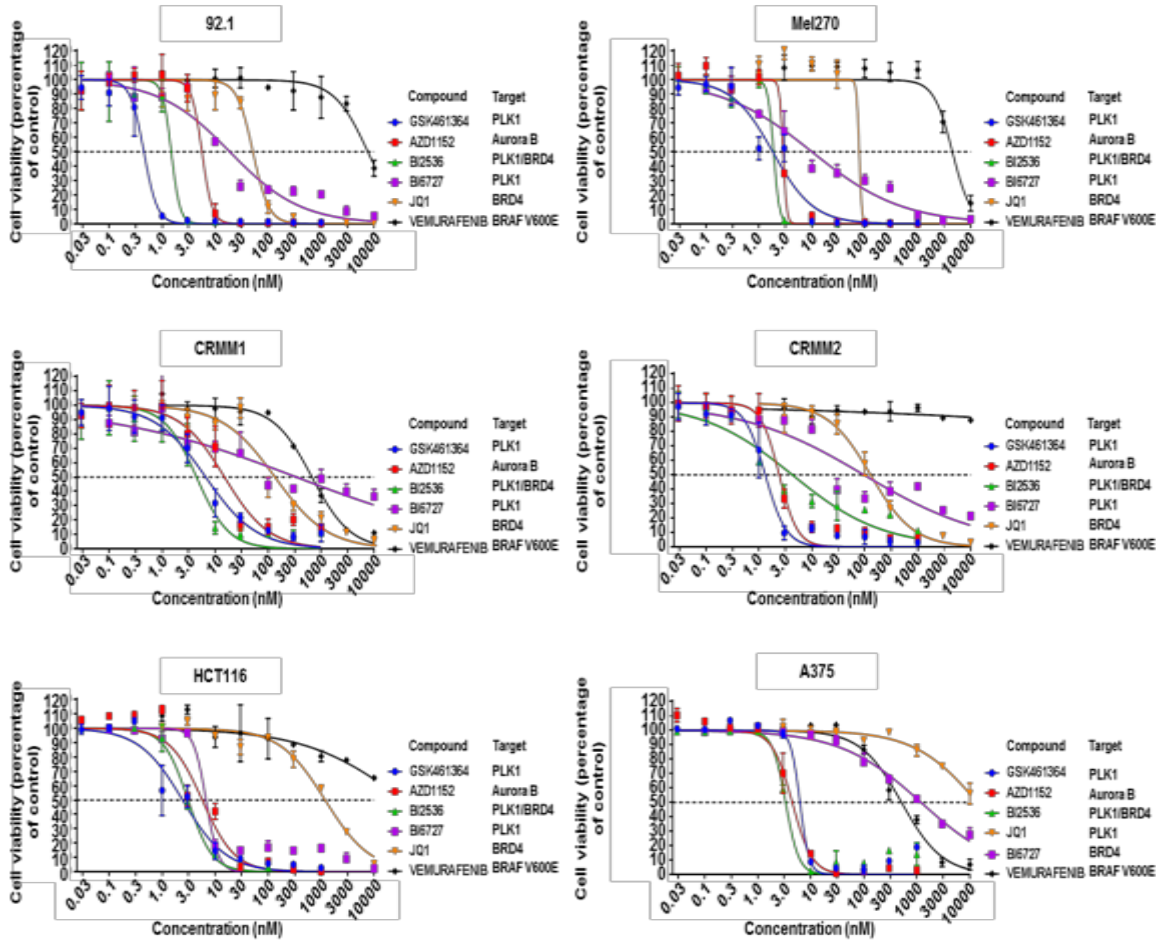
Supplementary Figure 3



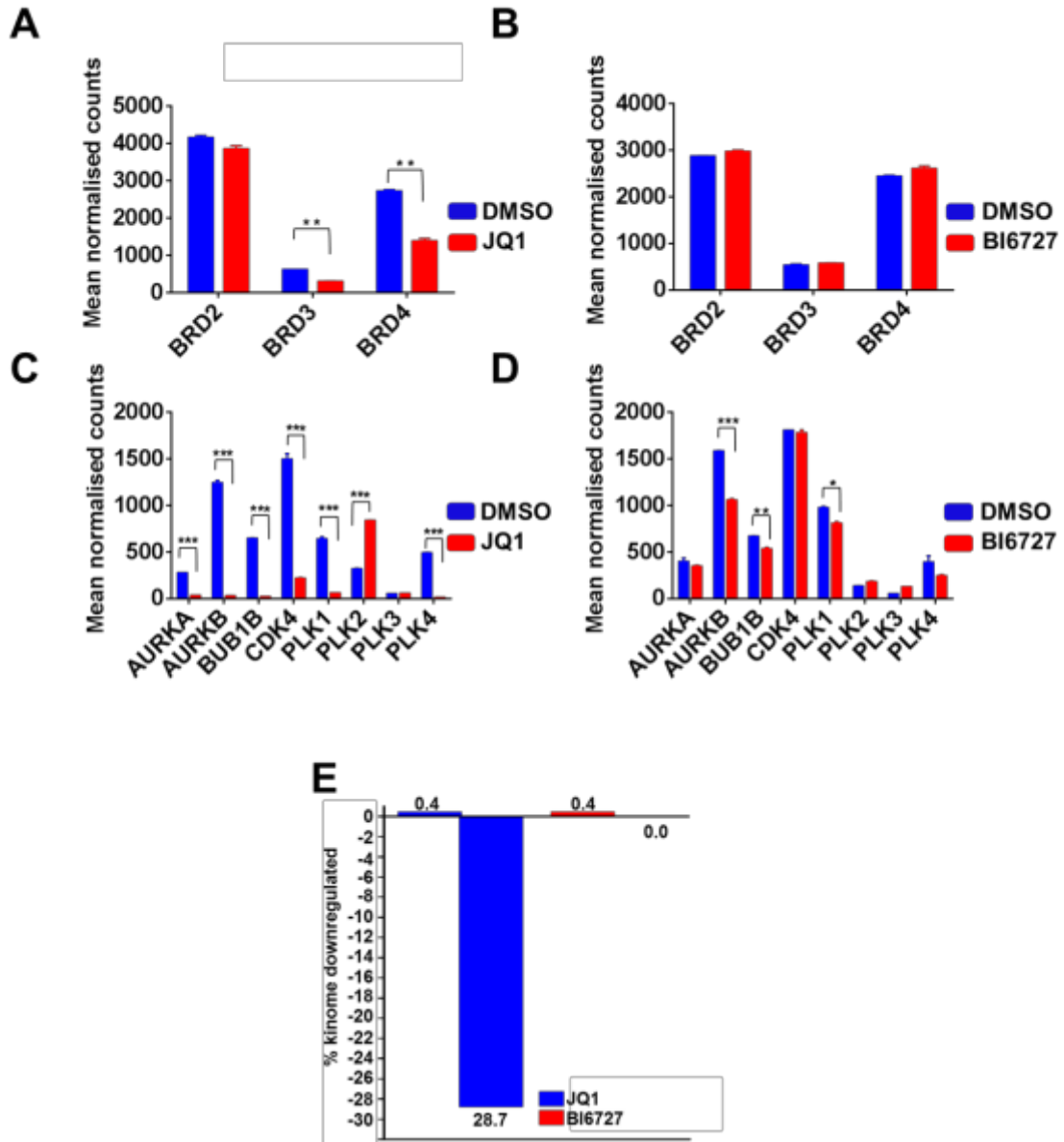
Supplementary Figure 4



Supplementary Figure 5



Supplementary Figure 6



SUPPLEMENTARY FIGURE LEGENDS

Supplementary Table 1. Genetic analysis of cell lines evaluated in this study.

Chromosome and mutational status of common melanoma-associated genes in experimental cell lines.

Supplementary Figure 1. Rank order of kinase mRNAs in UM, CoM and control human cancer cell lines.

In terms of normalised counts, the most highly expressed human kinase mRNAs in the indicated cell line are quantified, beginning with the highest, with BET-domain proteins BRD2 and BRD4 included for comparison. The rank mRNA levels of BRD2 (green), BRD4 (red), CDK2 and TAOK3 (pink) mRNAs are indicated.

Supplementary Figure 2. Rank order of kinase mRNAs from archival UM samples.

(A) Kinome mRNA levels from three individual UM patient samples were quantified by NanoString and the highest 10% are shown in the figure, starting with the highest. BRD2 (green), BRD4 (red), CDK2 and TAOK3 (pink) mRNAs are indicated. (B) The mRNA levels of CDK2, TAOK3, EGFR, BRD2 and BRD4 from each the three specific samples in (A), and an additional 6 patient samples, were quantified. Chromosome 3 status (monosomy (M3) or disomy (D3)) for each sample was determined by is shown.

Supplementary Figure 3. High levels of CDK2 protein and mRNA are not predictive for inhibitor sensitivity

MTT assays were performed after 4500 cells were incubated in triplicate (N=2) with increasing concentrations of (A) SNS032 or (B) palbociclib in mid-log ranges between 1 nM and 10 μ M for 5 days, and compared to 0.1% (v/v) DMSO controls.

Supplementary Figure 4. JQ1 represses CDK4 mRNA and induces a G1 cell cycle arrest in UM cells.

(A) Normalised transcript levels of *CDK4* mRNA measured after exposure to DMSO, JQ1 or JQ1(-) with standard deviation error bars. Statistical significance between JQ1 treated cells and controls was demonstrated using paired t-tests. *= $p < 0.05$, **= $p < 0.01$, ***= $p < 0.001$. (B) 92.1 and OMM1 UM cells were exposed to 1 mM JQ1 for 48 hours then stained with propidium iodide (PI). DNA content was measured by flow cytometry and the percentage of cells in each phase of the cell cycle was estimated. (C) 92.1 and OMM1 lysates were resolved by SDS-PAGE and protein levels of Cyclin D1 determined by western blotting. α -tubulin was used to control for protein loading.

Supplementary Figure 5. Comparative analysis of targeted compounds in cell models.

The indicated cell lines were incubated with increasing concentrations of compounds between the mid-log ranges of 0.03 nM to 1 μ M (GSK461364, AZD1152, BI2536 and BI6727) or 1 nM to 10 μ M (vemurafenib and JQ1) and compared to 0.1% (v/v) DMSO controls. Cytotoxicity was determined by SRB assay.

Supplementary Figure 6. Distinct transcriptional effects of JQ1 and BI6727 in 92.1 cells

Quantified mRNA counts (mean \pm S.D.) of BRD family members after incubation with either (A) JQ1 or (B) BI6727. (C) Mitotic kinases (including the PLK family, which are targets of BI6727) were quantified after exposure to JQ1 or (D) BI6727. Statistical significance between compound-treated cells and the controls was assessed using paired t-tests. $*=p<0.05$, $**=p<0.01$, $***=p<0.001$. (E) mRNAs were quantified using NanoString technology, following JQ1 or BI6727 exposure and compared to DMSO-treated controls. The number of kinases whose expression changed by more than 2 fold were counted and converted to a percentage of the 522 kinases analysed. Kinases with increased or decreased expression relative to untreated controls are shown on the positive or negative axis respectively.